pathogen has been on the scene, fungicides have become increasingly ineffective against it. "In Central America, we need to spray once a week," says Aguilar Moran.

Black sigatoka is on the march in Africa, too, but it's just one of many threats to that continent's bananas. Frison, now the director general of Bioversity International, a nonprofit that coordinates research into improving the lot of bananas and other crops, says that in Eastern Africa, farmers have been growing bananas on the same plots for 100 years, which has led to a decline in soil fertility. "They can't grow bananas anymore," he says.

Banana biodiversity is also suffering: Due to globalization, African farmers in-creasingly grow only the varieties they can sell at the market, says Frison. Whereas the average farmer used to cultivate a dozen varieties, now he only grows four or five. Without human-assisted propagation, the rest of the varieties disappear. That means less raw material for breeders like Aguilar Moran.

Consumed. Bananas are a staple food in developing countries, but they are also victims of fungal diseases.

CREDITS (TOP TO BOTTOM): JOSE FUSTE RAGA/CORBIS; JUAN FERNANDO AGUILAR MORAN

The forgotten fruit

Of course, diseases and loss of biodiversity plague many of the world's other major food crops. But they have one distinct advantage over the banana: People care about them. The United States, China, and other countries have spent far more on rice, corn, and wheat than they have on bananas. In 2008, for example, the U.S. Agency for International Development funded about $9 million in rice research but just over $1 million in banana research. "It puzzles us," says Richard Markham, a program director at Bioversity International. Most funding agencies in developed countries don't take the Cavendish seriously, he says, and they don't realize that the vast majority of other bananas are a staple food source for millions. (In Uganda, the word for "banana" and "food" is the same.) "It's hugely neglected and underinvested."

Even the banana industry doesn't seem to care. Banana suppliers Dole Food Co. and Chiquita Brands International have largely stayed out of banana research for the past 20 years, says Markham, although Chiquita has recently begun funding FHIA. Critics say the companies are shortsighted and that they haven't learned the lessons of the Gros Michel disaster. (Representatives for Dole and Chiquita did not return phone calls for this article.) Regardless, the assumption that these companies are looking out for the banana has kept the public sector away, says Markham.

The lack of attention has dealt a huge blow to efforts to sequence the banana. Frison hoped the 2001 meeting at NSF would mobilize a big investment, but nobody jumped on board. "We only found small and scattered money," he says. Roux took over for Frison in 2003, and over the next 4 years the Global *Musa* Genomics Consortium collected members—37 institutions in all, including the J. Craig Venter Institute and the Max Planck Institute for Chemical Ecology—but not much funding.

Hoping for U.S. support, the consortium approached the U.S. Department of Energy's (DOE's) Joint Genome Institute (JGI) in January 2008. JGI has a program to which research communities can apply to have the DNA of their favorite organism deciphered. Roux says JGI seemed enthusiastic about the banana. But this summer, the consortium learned that it didn't make the cut. Duckweed and sea grass did.

JGI's James Bristow says these species fit better into DOE's mission of investigating species for alternative fuels and bioremediation, though he admits to being disappointed by the reviewers' decision. "It's an important and endangered worldwide food crop," he says. "There's no question that this genome should be sequenced."

Jane Silverthorne, who headed NSF's Plant Genome Research Program from 1999 to 2007, says the bigger problem may be that the banana community is just not as well-organized as other crop communities. "It's small and fragmented," she says. Some banana proponents would rather see money put into subsistence farming than sequencing, Markham points out, "and even within molecular biology, some say we don't need the entire sequence—or that we should wait until the cost of sequencing comes down."

Nonetheless, Markham says it would be a "huge boost" for banana researchers to have the sequence. The trick is finding someone who will step up to fund it.

Slipping into the future

That someone might just be France. When members of the banana consortium gathered at the JGI workshop in January to present their sequencing plan, they got an unexpected boost from Francis Quétier, then deputy director of French sequencing giant Genoscope. Quétier announced that his institute would do half the work needed to generate a reliable sequence by covering the genome four times over. It had settled on a close relative of the Cavendish with only two sets of chromosomes. "Everyone cheered wildly," says Markham. But there was a catch: The French National Research Agency (ANR) would fund the project only with help from an international partner. When JGI subsequently passed on the banana, "the whole thing looked like it would unravel," Markham says.

Now Quétier, who recently became a program coordinator in genomics at ANR, says the agency is about to announce that it will fund the project anyway—and that it plans to sequence the entire genome. "We are at the beginning of the story," he says. "I'm very optimistic."

James Dale can't wait. A banana biotechnologist at the Queensland University of Technology in Brisbane, Australia, Dale has been trying to develop a better banana for 12 years through genetic modification. Once the sequence reveals the full range of genes in banana, he says, biotechnologists like him will be a step closer to using the banana's own genes to, say, boost disease-resistance.

That's not all. With the sequence, basic researchers can do comparative genetics with other crops and figure out how bananas got so strange in the first place. Even traditional breeders like Aguilar Moran will benefit: Molecular markers found in the genome will help them home in on traits of interest and better select varieties for crossing. "A tremendous amount of information will come out of this," says Dale.

Frison is also optimistic. As he did in 2001, he's predicting that the banana genome is within reach—and with it a brighter future for the fruit. "We've reached a turning point," he says. Bristow thinks that Frison might be right this time. "Once you've got a little bit of data, it starts to get interesting," he says. "Nothing rallies a community like some progress."

–DAVID GRIMM

LETTERS

edited by Jennifer Sills

European Union and NIH Collaborate

THE NATIONAL INSTITUTES OF HEALTH (NIH) AND THE EUROPEAN Commission (EC) recently decided to reinforce our mutual interest in scientific collaboration. We believe that greater trans-Atlantic cooperation and smarter competition in science will lead to faster breakthroughs in health research and ultimately to a better quality of life for the citizens of the world.

Partners. Former NIH Director Elias Zerhouni (left) and European Commissioner for Science and Research Janez Potočnik (right) make their new collaboration official.

The NIH has a long tradition of funding collaborations between U.S. and European scientists. To this end, the NIH recently clarified its policies for funding global collaborations (*1*). And on 3 September 2008, the European Commission published a new call for proposals within the health theme of its Seventh Framework Programme for Research and Development (*2*). For the first time, the EC has announced that researchers working in U.S. institutions are eligible not only to participate in EC-supported research projects but also to receive funds from the EC if they are part of a consortium with European Union (EU) investigators.

We live at a time of great scientific opportunity, where global collaborations are essential for facilitating scientific discoveries aimed at improving public health. As science has become more complex, so has the need for both specialization and multidisciplinary approaches to problem-solving. While discovery increasingly depends on a new level of collaboration, it also depends on expertise, which may not reside within one country or even within one continent. A prime example of global collaboration is the tremendously successful Human Genome Project, which reached its goals ahead of time and under budget. Similarly, global collaboration is essential to the conduct of clinical trials and genetic research, where disease prevalence in a given region enables research that could otherwise not be conducted in the confines of a single country.

We hope that our initiative, aimed at opening our research programs, will serve as a launch pad for wider and more intense U.S.-EU cooperation in health as well as in other areas of research. This is a historic step for our institutions today, and we are confident that it will also prove to be a significant step for the future of science.

ELIAS A. ZERHOUNI[1] AND JANEZ POTOČNIK[2]

[1]Former Director, National Institutes of Health, Bethesda, MD 20892, USA. E-mail: zerhoune@mail.nih.gov. [2]European Commissioner for Science and Research, Science and Research European Union, European Commission, Brussels B-1049, Belgium. E-mail: janez.potocnik@ec.europa.eu

References

1. Updates and Reminders on NIH Policy Pertaining to Grants to Foreign Institutions, International Organizations and Domestic Grants with Foreign Components (http://grants.nih.gov/grants/guide/notice-files/NOT-OD-09-010.html).
2. Seventh Research Framework Programme (http://cordis.europa.eu/fp7/dc/index.cfm).

Skeptical of Assisted Colonization

O. HOEGH-GULDBERG *ET AL.* ("ASSISTED COLonization and rapid climate change," Policy Forum, 18 July, p. 345) outlined a decision-tree framework for conservationists to use when considering the fate of species endangered by climate change. Although the likelihood of species extinction may require consideration of drastic action, there are several reasons to be skeptical of the assisted colonization proposal: (i) A number of within-continent or within–"geographic region" introductions, including intentional ones, have proved calamitous for the recipient ecosystem (*1*–*3*). (ii) Other short-distance, regional-scale incursions across breached biogeographic barriers have also had negative consequences [such as the migration of marine species across the Suez Canal that is known as the Lessepsian migration (*4*)]. (iii) A potential recipient area would have to be deemed of much lesser conservation value than the (single) species being assisted. Such a decision would be the antithesis of the flagship species approach currently adopted by conservationists. (iv) The resilience of a recipient region, already experiencing climate-induced stress itself, is unlikely to be assisted or enhanced by an introduced species. (v) The extent of knowledge required to provide detailed scientific understanding of the potential consequences of assisted colonization should not be underestimated; there are good reasons for bioinvasion ecologists to avoid experiments that require introducing potentially invasive propagules to uninfected areas, and regulations require secure retention of nonnative propagules for laboratory experiments. (vi) There already exists an approach to assist the persistence of endangered species: collaborative captive breeding programs of zoos and wildlife parks.

Any strategy to combat the negative impacts of a global phenomenon like climate change requires comprehensive frameworks. A species-by-species approach such as assisted colonization may be an overwhelming endeavor and is likely to encounter insurmountable policy conflicts between proponents and recipient regions. Such large-scale, manmade interference with species distributions in the wild does not have a glorious history and may prove a step too far as

CREDIT: MICHAEL SPENCER/NIH

HIV's dynamic transcriptase

1059

Degradation parallels

1062

a hedge against extinction.

IAN DAVIDSON[1]* AND CHRISTINA SIMKANIN[2]

[1]Aquatic Bioinvasion Research and Policy Institute, Portland State University and Smithsonian Environmental Research Center, Portland, OR 97207, USA. [2]Department of Biology, University of Victoria, Victoria, BC V8W 3N5, Canada.

*To whom correspondence should be addressed. E-mail: idavidso@pdx.edu

References

1. S. J. Kupferberg, *Ecology* **78**,1736 (1997).
2. J. D. Olden *et al.*, *Biol. Invasions* **8**, 1621 (2006).
3. J. M. Mueller, J. J. Hellmann, *Conserv. Biol.* **22**, 562 (2008).
4. B. S. Galil, *Biol. Invasions* **2**, 177 (2000).

Assisted Colonization Won't Help Rare Species

THE POLICY FORUM "ASSISTED COLONIZAion and rapid climate change" (O. Hoegh-Guldberg *et al.*, 18 July, p. 345) spells hope for our attempt to avert the worst of today's climate-induced extinction crisis. Unfortunately, the framework that the authors proposed and the discussions preceding this (*1*, *2*) have oversimplified the process of assisted colonization. Species in need of such an intervention are often uncommon or rare and may be understudied. Introducing them to new locations may help them keep up with climate change, but most of the other threats they have been facing (such as disease and poaching) are not likely to be left behind (*3*, *4*). These may even be exacerbated when species are moved across national boundaries; distinct systems of governance and management can impede conservation efforts (*5*). As a result, the number of threatened species that qualify for such a measure is likely low.

Indeed, data from the Report "One-third of reef-building corals face elevated extinction risk from climate change and local impacts" (K. E. Carpenter *et al.*, 25 July, p. 560) show precisely that. Of the 231 coral species listed in threatened categories, 186 (81%) are rare or uncommon. Worse still, we have virtually no fundamental knowledge on the biology of 70% of these corals, complicating the decision to translocate them. Moreover, at least 35 of them are harvested for the coral trade (more than 1000 pieces per year). It would be hard to imagine that assisted colonization will improve their fate. I urge caution in committing species to such movements until we are fairly confident that this will do more good than harm.

DANWEI HUANG

Scripps Institution of Oceanography, University of California, San Diego, La Jolla, CA 92093, USA, and Department of Biological Sciences, National University of Singapore, 117543, Singapore. E-mail: huangdanwei@ucsd.edu

References

1. M. L. Hunter, *Conserv. Biol.* **21**, 1356 (2007).
2. J. S. McLachlan, J. J. Hellmann, M. W. Schwartz, *Conserv. Biol.* **21**, 297 (2007).
3. C. K. Dodd Jr., R. A. Seigel, *Herpetologica* **47**, 336 (1991).
4. T. D. Steury, D. L. Murray, *Biol. Conserv.* **117**, 127 (2004).
5. G. H. Copp *et al.*, *J. Appl. Ichthyol.* **21**, 242 (2005).

Where Species Go, Legal Protections Must Follow

THE POLICY FORUM "ASSISTED COLONIZAion and rapid climate change" (O. Hoegh-Guldberg *et al.*, 18 July, p. 345) proposes moving species outside their historic range to mitigate biodiversity loss induced by climate change. However, this approach will be successful only if legal policies, especially the implementation of the Endangered Species Act (ESA), change as well. Establishing a new population requires both availability of adequate habitat and strong legal protection.

Policy-makers should recognize that areas predicted by bioclimatic models to be the most suitable for a species in the long term should now be considered "essential for conservation" under ESA section 3 and therefore designated as critical habitat. This should occur even if these areas are not currently suitable for the species. Designation of new populations established by assisted colonization as "experimental" under ESA section 10(j) should be avoided; this provides weaker protection than exists for naturally occurring populations and will ultimately jeopardize the populations most critical to a species' long-term survival (*1*).

GUILLAUME CHAPRON* AND GUSTAF SAMELIUS

Grimsö Wildlife Research Station, Swedish University of Agricultural Sciences, Riddarhyttan 73091, Sweden.

*To whom correspondence should be addressed. E-mail: gchapron@carnivoreconservation.org

Reference

1. J. Kostyack, D. Rohlf, *Environ. Law Report.* **38**, 10203 (2008).

Letters to the Editor

Letters (~300 words) discuss material published in *Science* in the previous 3 months or issues of general interest. They can be submitted through the Web (www.submit2science.org) or by regular mail (1200 New York Ave., NW, Washington, DC 20005, USA). Letters are not acknowledged upon receipt, nor are authors generally consulted before publication. Whether published in full or in part, letters are subject to editing for clarity and space.

Response

THE LETTERS IN RESPONSE TO OUR POLICY Forum highlight many of the risks and consequences of making bad decisions, the logical consideration of which is the focus of our decision framework. The robust risk assessment framework we propose includes assisted colonization as one option among the full array of other strategies available to ecosystem managers.

Davidson and Simkanin correctly note that there are serious risks associated with ill-conceived assisted colonization, including the effects on source populations and the impact of translocated organisms at their destinations, which we mentioned in our Policy Forum. It is true that some short-distance translocations will be ill advised for recipient ecosystems and human communities, but the literature indicates that this risk escalates as organisms and ecosystems become more divergent. Evidently, there is no single strategy that will work across the board for all taxa, ecosystems, and regions. This is why we presented a decision framework rather than a prescription. The decision framework allows risks and benefits to be reviewed systematically, prior to any attempt to move species, communities, or ecosystems in response to climate change.

Neither Davidson and Simkanin nor Huang acknowledge that the risks of action must be balanced against the risks of inaction, which have frequently been high. During past periods of major climate shifts (changes of 6° to 10°C), the Earth experienced massive changes to the distribution and abundance of its biological systems. Recent temperature increases in many parts of the world exceed those seen during previous shifts (*1*). Redistribution in the modern world is also curtailed by human-dominated landscapes, which severely limit the total area of suitable natural habitats and create barriers to disper-

sal and migration. Even though the risks of translocation may be prohibitive in most situations, to ignore this option as species, communities, or ecosystems dwindle to extinction is not an option. Our framework systematically examines the advantages and risks of assisted colonization along with the full suite of other conservation options.

We agree with Chapron and Samelius that policy must be developed to recognize the importance of future habitats for organisms in a world that is changing from decade to decade. Equally important is the necessity for developing new policies that provide protection for newly transferred colonies, especially given that these are intended to be long-term as opposed to experimental translocations. Without the rapid evolution of policy in concert with innovative biological solutions, attempts to move species and communities to new locations ahead of climate change will be doomed to failure.

OVE HOEGH-GULDBERG,[1]* LESLEY HUGHES,[2] SUE MCINTYRE,[3] DAVID B. LINDENMAYER,[4] CAMILLE PARMESAN,[5] HUGH P. POSSINGHAM,[6] CHRIS D. THOMAS[7]

[1]Centre for Marine Studies, Australian Research Council Centre for Excellence in Reef Studies and the Coral Reef Targeted Research Project, The University of Queensland, St Lucia, QLD 4072, Australia. [2]Department of Biological Sciences, Macquarie University, NSW 2109, Australia. [3]Australian Commonwealth Scientific and Industrial Research Organisation (CSIRO) Sustainable Ecosystems, Post Office Box 284, Canberra, ACT 2601, Australia. [4]Fenner School of Environment and Society, The Australian National University, Canberra, ACT 0200, Australia. [5]Department of Integrative Biology, University of Texas, Austin, TX 78712, USA. [6]The Ecology Centre, Centre for Applied Environmental Decision Analysis, The University of Queensland, St Lucia, QLD 4072, Australia. [7]Department of Biology, University of York, Post Office Box 373, York YO10 5YW, UK.

*To whom correspondence should be addressed. E-mail: oveh@uq.edu.au

Reference

1. O. Hoegh-Guldberg *et al.*, *Science* **318**, 1737 (2007).

TECHNICAL COMMENT ABSTRACTS

COMMENT ON "Ancient Asteroids Enriched in Refractory Inclusions"

Dominik C. Hezel and Sara S. Russell

Sunshine *et al.* (Reports, 25 April 2008, p. 514) reported that certain asteroids contain 30 ± 10 volume percent calcium- and aluminum-rich inclusions (CAIs). We contend that the amount of CAIs in CV chondrites is two to three times as low as the 10 volume percent assumed by the authors; thus, we question whether the CAI-rich bodies they studied are indeed older than known asteroids or formed before the injection of ^{26}Al into the solar nebula.

Full text at www.sciencemag.org/cgi/content/full/322/5904/1050a

RESPONSE TO COMMENT ON "Ancient Asteroids Enriched in Refractory Inclusions"

J. M. Sunshine, H. C. Connolly Jr., T. J. McCoy, S. J. Bus, L. M. La Croix

Although the exact abundance of phases in carbonaceous chondrites remains debatable, a potentially lower absolute abundance of calcium- and aluminum-rich inclusions (CAIs) in the Allende meteorite does not change our fundamental conclusion. In a relative comparison, CAI-rich asteroids contain two to three times as many CAIs as the most CAI-rich meteorites. These asteroids are therefore greatly enriched in the earliest solar system materials and remain enticing targets for future exploration.

Full text at www.sciencemag.org/cgi/content/full/322/5904/1050b

CORRECTIONS AND CLARIFICATIONS

News of the Week: "Chinese cave speaks of a fickle sun bringing down ancient dynasties" by R. A. Kerr (7 November, p. 837). The stalagmite sample analyzed was 0.12 meters long, not 1.2 meters long as reported.

PALEONTOLOGY

Reading Behavior from the Rocks

Sören Jensen

Adolph Seilacher has made substantial contributions to sedimentology, taphonomy, functional morphology, and more recently to the interpretation of Ediacara-type fossils, but it is with ichnology (the study of trace fossils) that his name is most closely associated. Trace fossils—burrows, tracks, trails, and other evidence of organism-sediment interactions preserved in the rock record—are unique in that they can provide direct evidence of how animals lived millions of years ago, sometimes recording events lasting a few minutes or less. No one has been quite so successful in bringing trace fossils to life as Seilacher, and the long-anticipated *Trace Fossil Analysis*, which grew out of courses he gave at Tübingen University, offers an excellent introduction to his approach.

Trace Fossil Analysis
by Adolf Seilacher
Springer, Berlin, 2007. 240 pp. $69.95, £38.50. ISBN 9783540472254.

One of the book's plates includes a Sherlock Holmes–like silhouette. This is a reasonable allusion to Seilacher's ability to recreate a scenario of trace producer and behavior on the basis of evidence that may at first seem unpromising—for example, in deducing the "adventures of an Early Cambrian trilobite" from faint scratches on a bedding plane. Seilacher's ichnological publications span half a century and have played a large role in shaping the field. They are characterized by an economic and precise prose, also found in the book, but more than anything else what sets them apart are his drawings. It is therefore fitting that Seilacher structured *Trace Fossil Analysis* around his sketches and diagrams of distinctive and representative ichnogenera. These are arranged in 75 plates, each accompanied by about one page of text ("in the form of extended captions"). The plates and text are grouped into chapters with titles such as "Burrows of Short Bulldozers," "Deep-sea Farmers," and "*Cruziana* Stratigraphy." Through his discussions of informative examples, Seilacher addresses such topics as the application of trace fossils in environmental studies, the study of trilobite trace fossils, and the analysis of deep-sea trace fossils.

Readers already acquainted with Seilacher's publications will find much that is familiar, but the book also contains a number of new illustrations and the text is sprinkled with fresh insights and thoughts. For example, the section examining the evidence for pre-Ediacaran trace fossils includes images and discussion of the 1.7-billion-year-old (1.7-Ga) Sterling biota of western Australia (*1*). Here Seilacher also mentions a new take on the Chorhat "worm burrows" (circa 1.5 Ga) from India. He now suggests foam menisci as an alternative to his earlier interpretation (*2*) that these structures were made by wormlike animals even though they are much older than the presumed origin of metazoans.

In a text as wide-ranging as this, there are of course details with which not everyone will agree. One such instance appears in the chapter "Pseudo-Traces," where Seilacher interprets *Protospiralichnus* from the Early Cambrian of Siberia as a system of concentric microfaults. Having had the opportunity to examine this material in Moscow, I agree with the original interpretation of this structure as a trace fossil resulting from concentrated circling motion (a type of trace fossil commonly known from Cambrian strata as "*Taphrhelminthopsis*" *circularis*).

In the preface, Seilacher explains that the book is not intended to be a comprehensive text on ichnology. Instead, he aims for it to encourage the training of observational skills and of a "method of morphological thinking in terms of processes that could easily be transferred to any other subject matter." Nevertheless, the book will prove an indispensable aid to anyone teaching trace fossils at the university level. To that end, the annotated reference lists occurring at regular intervals throughout the book will be quite helpful. The emphasis is heavily on the trace-making activity of marine invertebrates in soft sediments, but there are also sections on vertebrate traces and on various sedimentary structures that might mistakenly be attributed to the activity of organisms. Seilacher includes the majority of the more common and meaningful ichnogenera, although the naming of trace fossils is not an important theme of the book. (It should also be noted that the criteria for defining ichnotaxa vary widely among different trace fossil workers.) The author does not treat trace fossils on hard substrates, and he refers readers to other sources for discussion on ichnofabrics—the broader look at the sediment structure resulting from bioturbation and an increasingly important branch of trace fossil analysis over the past several decades.

Trace Fossil Analysis will be cherished by ichnologists, even though they already know what to expect. But it will be particularly

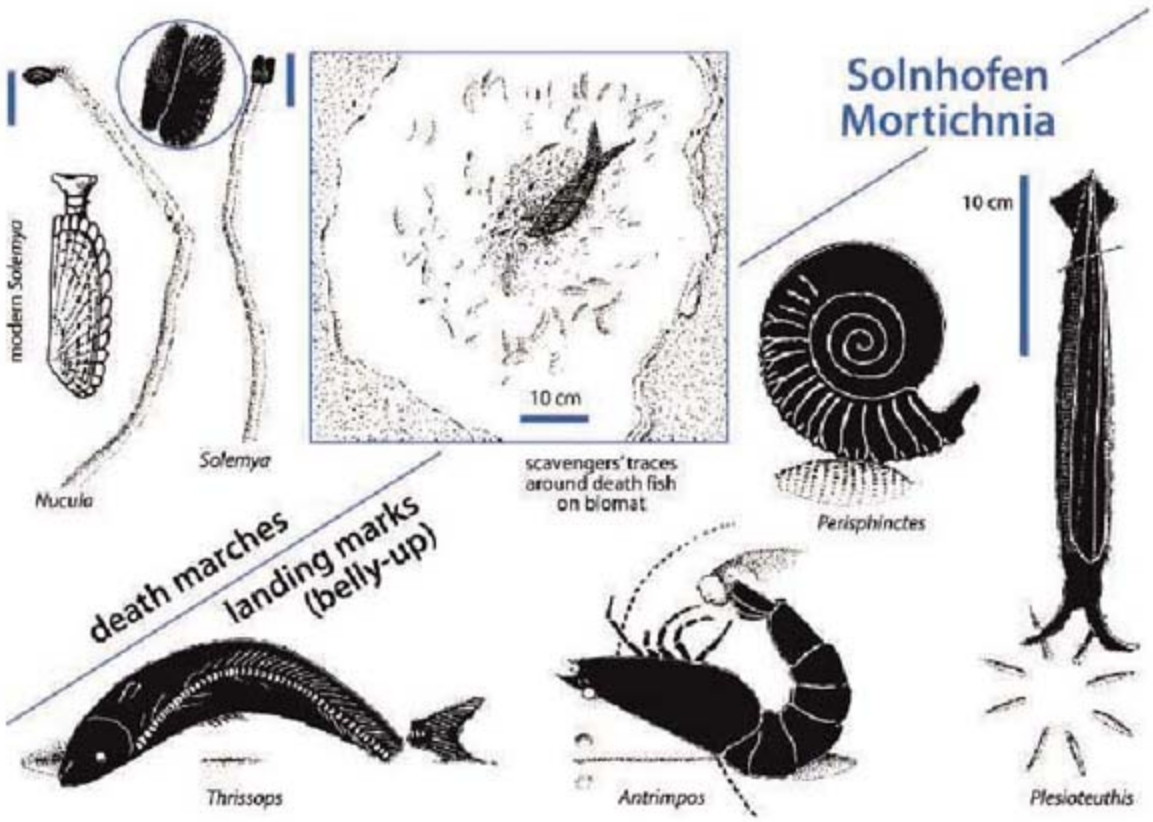

CREDIT: ADOLF SEILACHER/FROM *TRACE FOSSIL ANALYSIS*

Solnhofen stories. Many of the biogenic structures in the Upper Jurassic lithographic limestones from southern Germany record "the last movements (or even postmortem convulsions) of the trace makers preserved together with them."

The reviewer is in the Área de Paleontología, Facultad de Ciencias, Universidad de Extremadura, 06071 Badajoz, Spain. E-mail: soren@unex.es

handy to nonspecialists, who may not have the time, wish, or opportunity to track down Seilacher's original publications (some of which are in hard-to-find volumes). Nonspecialists should, however, keep in mind that such are the communicative powers of Seilacher's drawings and text that one can easily forget that these are interpretations—albeit ingenious ones and probably more often than not correct. This stimulating book documents the wonders that can be achieved by the eye and pen of a fertile mind.

References

1. B. Rasmussen, S. Bengtson, I. R. Fletcher, N. J. McNaughton, *Science* **296**, 1112 (2002).
2. A. Seilacher, P. K. Bose, F. Pflüger, *Science* **282**, 80 (1998).

10.1126/science.1166220

After Sputnik. Lee DuBridge (second from the left) and Vice President Richard Nixon hold a model of Explorer 1 at Caltech's Jet Propulsion Laboratory (1958). DuBridge would later serve as Nixon's science adviser to the president.

SCIENCE POLICY

What Can Science Do for the President?

Gregory A. Good

Consider a tale of two United States presidents and their approaches to science policy advice. The first preferred advisers who honestly disagreed with him and with each other, but who advised him with the best interests of the country at heart. The second preferred advisers who told him what he wanted to hear. The first preferred advisers who were skeptical of technological fixes; the second, advisers who thought technology could answer most challenges. The first preferred advisers with backgrounds in academia; the second, advisers from industry. The first president doubted the advice of ideologues and religionists; the second used their advice to form science policy on issue after issue. The first respected free and open debate; the second formed policy behind closed doors and presented carefully censored reports to the public.

The second U.S. president above is clearly George W. Bush. Readers may be surprised, however, to find that the first is General Dwight David Eisenhower, who in 1957 established the President's Science Advisory Committee (PSAC).

In Sputnik's Shadow
The President's Science Advisory Committee and Cold War America

by Zuoyue Wang

Rutgers University Press, New Brunswick, NJ, 2008. 477 pp. $49.95. ISBN 9780813543314.

Zuoyue Wang's *In Sputnik's Shadow: The President's Science Advisory Committee and Cold War America* reminds us in rich detail of various ways in which U.S. presidents, especially in the mid- and late 20th century, have obtained advice on science. Wang (a historian at California State Polytechnic University, Pomona) focuses on the period from the Eisenhower administration to that of Richard Nixon but glances backward and forward. Despite these glances, his book is neither a prescription nor a diatribe but rather a careful and nuanced historical analysis. Readers looking for simple answers to where American science policy should go next need to look elsewhere. In Wang's book they will instead find a fully developed and complex historical analysis.

Eisenhower created PSAC in the midst of the Cold War, soon after the Soviet Union's October 1957 launch of Sputnik. Eisenhower charged the committee with advising him mainly on science and technology relevant to defense and nuclear weapons—or more to the point, relevant to arms control. Presidents before Eisenhower had sought advice from scientists, through either the National Academy of Sciences or ad hoc arrangements, but PSAC was intended to regularize the process. In addition, during World War II the Office of Scientific Research and Development, the Radiation Lab, and the Manhattan Project had fundamentally altered the culture of physics in the United States.

A recurrent theme throughout the book concerns the dual nature of science in American politics: science in policy versus policy for science. This seemingly cryptic phrase has a simple, direct meaning. Presidents realize that to forge policies regarding defense, energy, etc., government needs competent advice about science and technology, and PSAC provided such expert advice. Scientists have another interest, namely the funding and promotion of their research and their institutions. As Wang encapsulates the distinction: what can science do for the government versus what can government do for science? PSAC scientists recognized that these two perspectives are inextricably linked, and committee members often linked the country's policy interests with the self-interest of their science. Aware of the distinction, Wang narrates many efforts of PSAC to "blur the boundary."

Wang also emphasizes the balance that PSAC scientists tried to maintain between technological enthusiasm and technological skepticism. They insistently included technological limitations, environmental and social risks, and policy implications in their analyses—as in those regarding nuclear-powered airplanes, the supersonic transport, antiballistic missiles (ABM), and pesticide use. Wang notes "theirs was not an argument against technology, but one for appropriate technology, for a broadened concept of technological rationality that encouraged technological development not for its own sake but for its benefits in achieving social, political, cultural, and economic goals in a democratic society."

The demise of PSAC came during the Nixon years, in large part through tensions magnified by the ABM debate. Nixon first distanced himself from his science adviser, Lee DuBridge, and ultimately, just weeks after the 1972 election, decided to dissolve the Office of Science and Technology and with it the committee. The decision then took six months to be finalized. As Wang suggests, PSAC's closing occurred at least in part because Nixon did not want the broader technological rationality that previous presidents had favored. He resented disagreement from his advisers.

Wang provides the scientific community and policy-makers with a most timely reminder of the positive roles that scientists can play in an open society. We can only hope that Barack Obama will turn a page and not let ideology, personal beliefs, or party politics interfere with his seeking of sound science advisement. *In Sputnik's Shadow* offers a history that both policy-makers and scientists should heed well.

10.1126/science.1165661

The reviewer is at the Department of History, West Virginia University, Morgantown, WV 26506–6303, USA. From January 2009, he will be at the Center for History of Physics, American Institute of Physics. E-mail: greg.good@mail.wvu.edu

CREDIT: PHOTO 80-H-116/NASA

OCEANS

Smithsonian Swims in New Direction

Lekelia D. Jenkins

Sant Ocean Hall

Carole Baldwin, Sharon Katz Cooper, Brian Huber, Jill Johnson, Elizabeth Musteen, and Michael Vecchione, Exhibit Team

National Museum of Natural History, Smithsonian Institution, Washington, DC.
http://ocean.si.edu/ocean_hall/

Although many factors led me to become a marine scientist, one was definitely the Smithsonian Institution's National Museum of Natural History (NMNH). I fondly remember childhood class trips to the aging marine hall. The exhibition was dim and musty, but the sheer wealth of knowledge held there made each visit a fresh and educational experience (even as an adult). I wondered whether the Sant Ocean Hall has the depth of knowledge to inspire a new generation of scientists as the earlier displays had inspired me.

Rare and wondrous but smaller than life serves as a good description of not only the giant squid highlighted in the new hall but also the exhibit itself. Although the display of two giant squid specimens is indeed worth seeing, the preserved quality of these fascinating and elusive creatures is disappointing. A plaque above the slightly decayed carcass of the larger, 7.3-m-long specimen explains that it has shrunk as a result of preservation and is substantially smaller than its original size.

Likewise, the heralded ocean-themed hall—a first for the Smithsonian—does not quite meet heightened expectations. The Smithsonian raised $80 million for the ambitious project, including $22 million from the National Oceanic and Atmospheric Administration (NOAA), the exhibit's cosponsor. At over 2100 m^2, the Ocean Hall is the NMNH's largest permanent exhibition. Nonetheless, it can display only a small portion of the Smithsonian's 30 million specimens of ocean organisms (the largest marine collection in the world). The material is organized around the themes of how the ocean has changed over time and how marine ecosystems vary across habitat types. Using 30 "human connections" stories (which are linked to critical ocean issues), the exhibit also attempts to show visitors that "the ocean is a global system essential to all life—including yours." However, because there is no clear path through the exhibit and the pithy signage is disparate and often poorly placed, the themes break down and the displays are incongruous.

The Ocean Hall incorporates a number of interactive video components that curators can update through the expected 30-year lifetime of the exhibit. For instance, one interactive kiosk simulates ocean management, allowing visitors to manipulate parameters such as fishing controls, aquaculture controls, and monitoring and then see the effects of their decisions on the ecosystem and stakeholders. The most frequently updated part of the hall will be the two Ocean Today Kiosks, video displays that offer visitors captivating two-minute summaries on a variety of contemporary ocean topics. These well-conceived kiosks, maintained by NOAA, will be regularly refreshed with new videos (30 story lines are currently in production), and they will soon feature a ticker-type crawl with the latest ocean news. But because they have poorly functioning directional speakers and are situated in an obstructed corner, the kiosks probably will not be able to shoulder the duty of keeping the entire Ocean Hall timely and relevant.

Visitors will be entertained by some impressive marvels, such as a living coral reef and a 14-m-long replica of Phoenix, a particular North Atlantic right whale, *Eubalaena glacialis*. The 1500-gallon coral aquarium houses fish, live coral, anemones, and other organisms that were all grown in captivity or collected in a sustainable manner. Visitors also cluster in engaging areas such as the Global Ocean Systems gallery. In this room, an animated six-foot sphere aptly tutors viewers on complex oceanic processes, such as the formation of the continents.

But these attractions are small islands of excitement in a sea of last-century displays of fossils, corpselike models, and pale dead fish in jars that museum-goers quickly pass. These attempts to incorporate the museum's extensive collection into the hall are disharmonious anachronisms, given the technological scaffold of the exhibit. A video or interactive program could help visitors place the specimens within the larger conceptual context of the display and understand the value of preserved specimens to science. By presenting more actively posed models (such as the exquisite model of a dumbo octopus, *Cirrothauma magna*, with tentacles coiled in midpropulsion), the exhibit could have worked in aspects of the biomechanics of marine organisms. Also, the designers might have borrowed from one of the best aspects of the museum's Mammal Hall, the use of specimens in lifelike assemblages to communicate ecological information. For example, grouping of models or specimens could have provided insight into food webs. The implicit as well as explicit imparting of information would have added depth to the exhibit, making it more appealing to a wider audience.

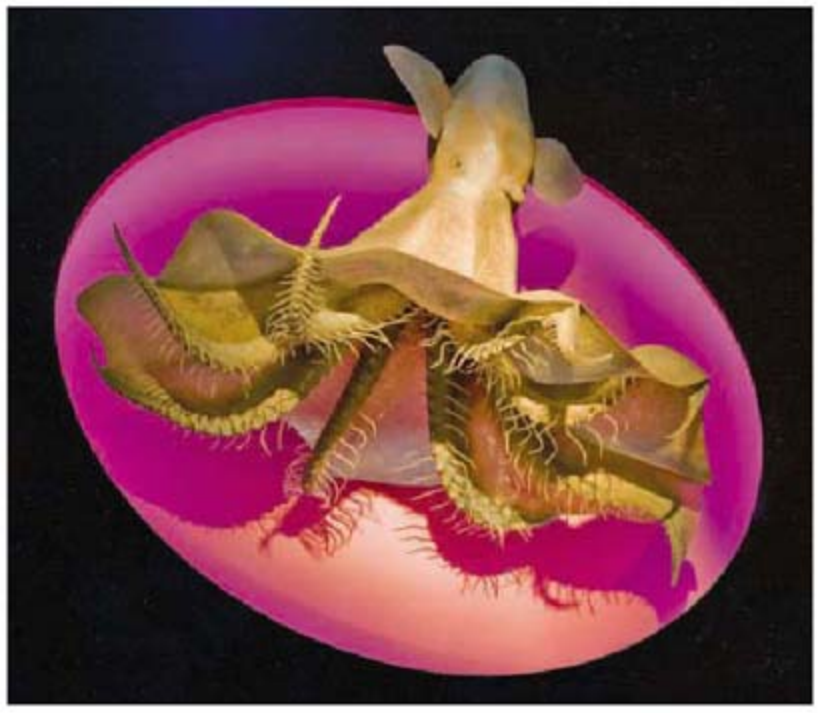

CREDIT: CHIP CLARK/NMNH, SMITHSONIAN INSTITUTION

Model display. The dumbo octopus *Cirrothauma magna*.

By far the highlight of the entire hall is the Ocean Explorer Theater. Here, in a video with vivid cinematography, a diverse cast of scientists describes with sincere awe their experience of discovery as they descend to the sea floor in a deep-sea submersible. The video moved me on an emotional level, reaffirming both why I love being a marine scientist and the powerful draw of the deep blue as our last natural frontier. I have no doubt that the theater and other effective parts of the exhibit will help inspire the next generation of marine researchers. The Sant Ocean Hall, although not all that I had anticipated, is still rare and wondrous.

10.1126/science.1167002

The reviewer is a AAAS Science and Technology Policy Fellow (http://fellowships.aaas.org/03_Directory/03_List_AZ.shtml#), 1220 East-West Highway, #216, Silver Spring, MD 20910, USA. E-mail: kiki.jenkins@gmail.com. The views expressed are the reviewer's own and do not represent those of any supporting organization.

RESEARCH ETHICS

Certificates of Confidentiality and Compelled Disclosure of Data

A recent court case suggests that the privacy of research subjects may not be fully protected by Certificates of Confidentiality.

Laura M. Beskow,[1,2*] Lauren Dame,[2,3] E. Jane Costello[4]

Ethical principles and professional codes of conduct require that researchers protect research participants' privacy, as well as the confidentiality of their data (*1*, *2*). Certificates of Confidentiality are intended to help meet these obligations by preventing forced disclosure of identifiable data during legal proceedings (*3*). A recent case indicates that the protection Certificates offer is uncertain.

Certificates are authorized by federal law and granted by units of the U.S. Department of Health and Human Services for research collecting information that, if disclosed, could have adverse consequences or damage subjects' financial standing, employability, insurability, or reputation. The current law states that with a Certificate, "persons engaged in biomedical, behavioral, clinical, or other research … may not be compelled in any Federal, State, or local civil, criminal, administrative, legislative, or other proceedings to identify such individuals" (*4*).

Although Certificates are commonly believed to offer "nearly absolute privacy protection" (*5*), there is a remarkable paucity of evidence on which to base such conclusions. In one of the only reported court opinions, *People* v. *Newman* (*6*), a Certificate successfully prevented disclosure of the identities of participants in a drug treatment program despite a grand jury subpoena in a murder investigation. Both sides in this case assumed that confidentiality protections granted under the law were absolute; the dispute focused on whether other legislation (*7*) repealed these protections. The Court held that the other legislation did not do so, but provided little analysis of the scope of a Certificate's protections.

We describe a criminal case that reached the North Carolina Court of Appeals, in which research data collected under a Certificate were subpoenaed by the defense in an attempt to impeach the credibility of a prosecution witness. The outcome raises concerns about the protections Certificates provide and has implications for research that depends on participants' confidence that sensitive information will be protected.

Case Presentation

In the early 1990s, Duke University Health System (DUHS) researchers began a longitudinal study of psychiatric disorders and the need for mental health services among rural and urban youth (the "Study"). Researchers obtained a Certificate from the National Institute of Mental Health because they planned to gather information about psychosocial adversities, substance abuse, illegal behaviors, and genetic traits.

The challenge to the Study's Certificate arose in 2004 from a criminal proceeding in which the defendant was charged with indecent liberties with a minor and statutory rape. His attorney believed that a prosecution witness was a Study participant and requested a court order directing DUHS to supply all Study records about the witness. The court granted this request, noting that the defendant was entitled to the records for any exculpatory evidence they might contain. Although the order directed that the records remain confidential unless used at trial or sentencing, it allowed them to be read by the state's chief investigating officer, the witness, the District Attorney's office staff, the defendant and his wife, the Public Defender's office staff, the Assistant Public Defender, and any expert the defendant or state might consult (*8*).

The full legal effect of Certificates of Confidentiality remains unclear.

The judge issued this order without knowledge of the Certificate; DUHS first learned of the attempt to obtain Study records upon receiving the subpoena. DUHS filed a motion for a protective order, asserting that the records were protected by a Certificate and should not be disclosed. DUHS also argued that the person whose records were sought was not the alleged victim; therefore, Study records were unlikely to contain exculpatory evidence. DUHS took no position regarding whether the witness was a Study participant. On the basis of its review of the motions, an affidavit from the Principal Investigator (PI), and arguments made at the hearing, the court vacated its initial order and granted DUHS' motion, but instructed DUHS to maintain a sealed copy of the records until the final resolution of the case.

A review of the hearing transcript (*9*) shows that the judge regarded the defendant's request to access Study records as a routine discovery motion and was unfamiliar with Certificates. He told DUHS that he had not realized "what kind of egg [he was] cracking open," but "obviously it had lit a fire under somebody." Further, although DUHS and the PI argued the critical importance of upholding the Certificate, the judge seemed most swayed by the argument that the defense was unlikely to find exculpatory evidence. Thus, despite the Certificate, the court weighed other interests and issued the protective order only after deeming the defendant's reasons for seeking the records insufficient.

The defendant was tried and convicted of all charges. Months later, the defendant's appellate lawyer filed a motion requesting access to the sealed records. A hearing was held before the same judge. This time, however, he ordered that the records be given to defense counsel and shared with the state, suggesting that it would be puzzling to ask the appellate court to decide if the records were relevant when the defense attorney arguing their relevance had never seen them (*10*). Arguments based on their contents could only be made in a separate sealed brief.

DUHS filed a notice of appeal, asserting

[1]Duke Translational Medicine Institute, Duke University, Durham, NC 27710, USA. [2]Duke Institute for Genome Sciences and Policy, Duke University, Durham, NC 27708, USA. [3]Duke University School of Law, Durham, NC, 27708, USA. [4]Developmental Epidemiology Program, Department of Psychiatry and Behavioral Sciences, Duke University Medical Center, Durham, NC 27710, USA.

*Author for correspondence. E-mail: laura.beskow@duke.edu

the Certificate and citing *People* v. *Newman* as particularly relevant, arguing that participants "must be given genuine assurances of confidentiality for investigators to obtain candid, meaningful, and wide participation in the study" (*11*). DUHS also argued that the defendant had failed to show that the documents were relevant to his defense. Pursuant to the court order, however, DUHS delivered the documents to the defendant's appellate counsel.

The defendant's brief contained a sealed appendix based on the Study records. In the unsealed portion, the defendant argued that *Newman* did not govern this situation because "[*Newman*] involves the State seeking information for use in a criminal prosecution as opposed to [this] case which involves a criminal defendant who has been afforded the Constitutional right to due process and confrontation to gain favorable and material information for his defense" (*12*). After hearing from DUHS and defense counsel, the Court of Appeals concluded that the Study records were not material. It vacated the order granting defense counsel access, but confidentiality had already been compromised. The Court specifically declined to consider DUHS' argument that the confidentiality of the records was statutorily privileged (*13*) and, thus, failed to address whether the Certificate would have protected the records, had they been material to the defendant's case.

Discussion

Certificates have gained prominence over the past decade. In 2002, the National Institutes of Health (NIH) announced a new policy encouraging broader use of Certificates (*14*). The National Cancer Institute recommends that biorepositories consider obtaining a Certificate (*15*), and NIH suggests as part of its data-sharing policy that Certificates be obtained for genome-wide association studies (*16*, *17*).

Given such reliance on Certificates, their effectiveness in preventing forced disclosure deserves rigorous evaluation. Because the U.S. case law system relies heavily on precedent, attorneys and judges will review previously decided cases when considering how to handle future legal demands for research data. In the case presented here, the Certificate helped convince the court, after vigorous legal intervention, to refrain from ordering broad disclosure of Study records, permitting instead restricted disclosure to attorneys for use under seal, but did not provide absolute protection. This highlights several important issues.

First, requests for research data may arise from legal proceedings unrelated to a study's focus. A PI or institution may unexpectedly receive a subpoena and need swiftly to engage a lawyer with appropriate expertise. When notified of a Certificate dispute, the Office of the NIH Legal Advisor provides citation to the statute and case law of which it is aware, but does not ordinarily involve itself in third-party litigation or provide legal advice to non-NIH entities.

Second, a Certificate is granted to the research institution, not the PI, and their interests may not be identical. In this case, the PI felt a moral obligation to protect participants' data; DUHS agreed and was willing to go to court. But an institution could decide that a costly legal battle is unwarranted or might be unwilling to defy court-ordered disclosure, even if the PI wants to do so.

Third, seeking to enforce a Certificate may result in some disclosure, even if data are not released. For some research, simply revealing the fact of a person's participation could itself cause adverse consequences. But institutions or investigators who refuse to follow a court order may be found in contempt, resulting in fines or imprisonment.

Fourth, parties in both criminal and civil lawsuits have rights to obtain material relevant to their case. Courts have broad powers to enforce these rights, and they attempt to resolve disputes by balancing each side's interests. When doing so, courts may give insufficient weight to society's interest in protecting research records. Further, when the attempt to obtain study records comes from a criminal defendant, a Certificate may be especially vulnerable if the records could affect a defendant's Constitutional rights to a fair trial or to confront and cross-examine witnesses. In this case, the court did not find that the facts implicated these rights, but a future case could raise the key question of when a defendant's Constitutional rights overcome the statutory protection offered by a Certificate. Finally, attempts by the government itself to obtain study records may raise particularly difficult challenges if the records are considered relevant to "national security." Since 9/11 and the passage of the Patriot Act (*18*), government agencies claim increasingly broad legal powers to obtain confidential information, and researchers may have great difficulty resisting disclosure.

Elucidating Certificates' practical utility in preventing compelled disclosure is a critical area for future study. Empirical evidence about how frequently research data are subpoenaed, and what happens when investigators assert a Certificate to protect data, is needed to help set realistic expectations about Certificates' role and value. In the meantime, the full legal effect of Certificates remains unclear, and caution is warranted when representing the impact of a Certificate to potential research participants.

References and Notes

1. Advisory Committee, Office for Human Research Protections, DHHS, *Recommendations on Confidentiality and Research Data Protections*, www.hhs.gov/ohrp/nhrpac/documents/nhrpac14.pdf.
2. National Commission for the Protection of Human Subjects of Biomedical and Behavioral Research, *The Belmont Report: Ethical Principles and Guidelines for the Protection of Human Subjects of Research* (Government Printing Office, Washington, DC, 1979).
3. Certificates of Confidentiality kiosk, NIH, http://grants.nih.gov/grants/policy/coc/.
4. *Public Health Service Act*, §301(d), 42 USC §241(d).
5. P. M. Currie, *IRB* **27**, 7 (2005).
6. *People* v. *Newman*, 32 NY2d 379, 298 NE2d 651, 345 NYS2d 502 (1973), *cert. denied*, 414 US 1163 (1973).
7. *Drug Abuse Office and Treatment Act*, 21USC §1101 (1972), Public Law 92-255.
8. *Order for Disclosure: Duke University Health System*, 29 July 2004.
9. Transcript of the hearing on Duke's Motion for Protective Order, 8 August 2004, p. 9.
10. Transcript of hearing on defendant's Motion for Review of Sealed Documents for Appellate Review, 25 April 2005.
11. Brief of Appellant/Subpoenaed Non-Party Duke University Health System, Inc., *State of North Carolina* v. *Bradley*, Case No. COA05-1167, NC Court of Appeals, filed 4 January 2006, p. 16.
12. Defendant-Appellee's Brief, *State of North Carolina* v. *Bradley*, Case No. COA05-1167, NC Court of Appeals, filed 4 January 2006, p. 17.
13. *State of North Carolina* v. *Bradley*, 179 NC App 551, 634 SE2d 258 (2006).
14. NIH announcement on Certificates of Confidentiality, http://grants.nih.gov/grants/guide/notice-files/NOT-OD-02-037.html.
15. *National Cancer Institute Best Practices for Biospecimen Resources* (NCI, NIH, Bethesda, Md, 2007); http://biospecimens.cancer.gov/global/pdfs/NCI_Best_Practices_060507.pdf.
16. *Policy for Sharing of Data Obtained in NIH Supported or Conducted Genome-Wide Association Studies* (GWAS), http://grants.nih.gov/grants/guide/notice-files/NOT-OD-07-088.html.
17. *Genome-Wide Association Studies (GWAS), NIH Points to Consider*; http://grants.nih.gov/grants/gwas/gwas_ptc.pdf.
18. *Uniting and Strengthening America by Providing Appropriate Tools Required to Intercept and Obstruct Terrorism Act of 2001* (*USA PATRIOT Act*), Public Law 107-56; 115 Stat. 272 (2001).

19. Supported in part by a grant from the NIH Clinical and Translational Science Award 1UL1RR024128-01 to Duke University. None of the authors has any conflict of interest, financial or otherwise, to declare. The authors thank J. McCall for editorial assistance and W. E. Freeman and L. E. Wolf for their input.

10.1126/science.1164100

CHEMISTRY

A Sideways Glance at Chemical Reactivity

Ultrafast spectroscopy allows us to see what happens to parts of a molecule not directly involved in a chemical reaction.

David A. Blank

Chemical reactions can often be described with surprisingly few variables, such as the highest energy barrier that is crossed and the nature of any brief stops in energy valleys along the way from reactants to products (see the figure, top panel). However, if the goal is to describe the choreography of chemical reactions and not just their rates, then a more complete description is needed that includes details such as whether the low-energy path widens or narrows as the reaction proceeds. The vast area between the stable points on this energy landscape dictates how a reaction takes place but is usually the most challenging piece to survey (see the figure, middle panel). On page 1073 of this issue, Takeuchi *et al.* (*1*) have reexamined the well-studied photoisomerization of stilbene, which is representative of a broad class of reactions that includes the photochemistry of vision (*2*, *3*). They map out previously hidden parts of the landscape through direct measurements of vibrational motions that occur in parts of the molecule that are not directly involved in the twisting of its double bond.

Starting around 1930, chemical reactions were described in terms of a potential energy surface that depicted how the energy of the molecules increases or decreases as bonds are broken, made, or deformed (*4*, *5*). Since then, much effort has been focused on finding ways to experimentally measure and computationally access the potential energy surface. Experimental studies are especially challenging in that the reacting molecules spend an extremely short time in the unstable regions, so the majority of the experimental observations are made on relatively stable molecules, which in some cases may be only the reactants and products. One analogy is that we are trying to describe what the players are doing at a tennis match on the basis of seeing the ball only when it hits the court or a racket, not when it is in flight.

The unstable regions can be probed by finding connections between what goes on there and more stable states. For example, optical spectroscopic methods excite the molecules from stable ground states to electronic excited states. The absorption of light can probe the difference between ground and excited states, and, if done at enough points on the ground-state surface, can allow us to map out the excited-state surface (see the figure, bottom panel). The reaction described by Takeuchi *et al.* actually takes place on the excited-state surface, and the ground-state surface provides an initial point of reference.

However, light absorption as a probe of the excited-state surface is limited in its access because the electronic changes occur on a much faster time scale than the response of the heavier nuclei. In the energy landscape, there is no movement along the horizontal directions that represent the distances between nuclei, so the transitions are described as "vertical." Thus, when *cis*-stilbene is photoexcited, the bonding pattern of its molecular orbitals now favors the trans arrangement around the double bond, and the nuclear coordinates try very quickly to "catch up" to this new stable point (to invoke our tennis match, this vertical transition is the racket deforming the ball). The accessible part of the upper surface, directly above the region of stability on the reference surface, is called the Franck-Condon region (illustrated as the green area in the bottom panel of the figure).

Spectroscopic methods that use more than one absorption or emission event, or both, and that have time resolution comparable to the time spent between the stable regions (10^{-13} to 10^{-12} s), can be used to probe directly the unstable regions of the potential energy surfaces (*6*). In the simplest implementation, a light pulse excites the reactant onto the upper surface in the Franck-Condon region. After a short delay, a second light pulse can be used to report on the progress of the reaction. This type of experiment can map the narrow path followed from 1 to 2, referred to as the reaction coordinate (illustrated with olive green in the figure). Takeuchi *et al.* take the next step by adding an additional dimension to the probe. They not only follow the reaction coordinate (the twisting of the double bond) but also measure changes in vibrations of other bonds in the molecule as the twisting proceeds.

Takeuchi *et al.* map the changes in topology around the reaction coordinate and fill

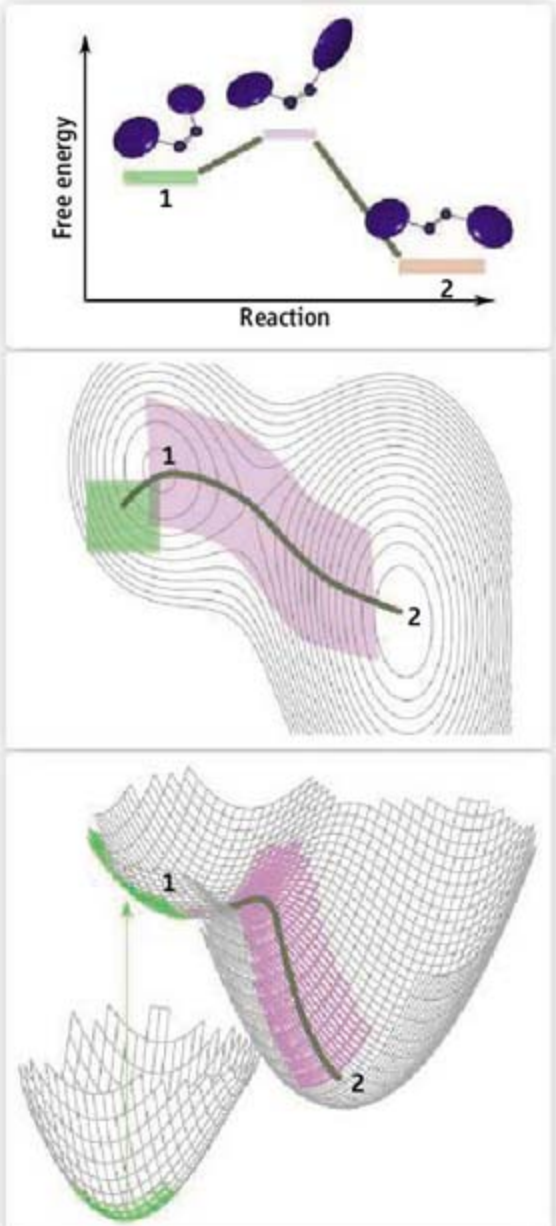

Degrees of realism in depicting chemical reactions. In all of these depictions, reactants (green regions) convert into products by moving quickly along a reaction coordinate (olive green and pink regions). **(Top)** A simple view of the energy barriers encountered along the reaction coordinate, which reflects the changes in one bond. For stilbene, the double bond must break to allow the phenyl rings to rotate, and the coordinate is the rotation angle. **(Middle)** The energy landscape for two degrees of freedom (more than one bond's motion) in a chemical reaction. Many more coordinates are often included, and depictions are slices in two dimensions. **(Bottom)** In a photoreaction, the changes in nuclear coordinates can occur along a second upper surface that represents an electronic excited state.

Department of Chemistry, University of Minnesota, 207 Pleasant Street SE, Minneapolis, MN 55455, USA. E-mail: blank@umn.edu

in the pieces of the landscape shown in pink. Their method is directly related to the time-resolved probing of vibrations by means of resonance Raman spectroscopy, as previously reported by Mathies and co-workers (*7*, *8*). The main difference is that Takeuchi *et al.* probe the vibrational motions in time rather than frequency, which has the practical result of lowering the frequency of the vibrations that can be accessed. Thus, they can observe the evolution of a vibrational motion of the carbon-carbon bond framework at frequencies around 200 cm^{-1} during the isomerization reaction, which represents nuclear motions with a period of 1.6×10^{-13} s.

This lower-frequency motion is similar in time scale to the motion along the reaction coordinate, and the curvature of the potential energy surface along these two dimensions is comparable. It provides details of how the phenyl rings move and twist as they settle into the extended trans conformation, which previously was viewed as a spectator to the motion rather than as part of the action. The complementary computational study in the report highlights the necessity of combining theory and experiment when mapping out these potential energy surfaces.

The report by Takeuchi *et al.* adds to our understanding of a specific class of chemical reactions by providing a new perspective on a model photoisomerization. Their study takes us beyond the question of "how fast" and to the more demanding question of "which way" at the level of the entire molecule. Although the method presented is technically demanding, it could be applied to a wide variety of photoinitiated reactions, including those that take place in complex environments such as proteins.

References

1. S. Takeuchi *et al.*, *Science* **322**, 1073 (2008).
2. C. Dugave, L. Demange, *Chem. Rev.* **103**, 2475 (2003).
3. M. V. der Horst, K. Hellingwerf, *Acc. Chem. Res.* **37**, 13 (2004).
4. W. Heitler, F. London, *Z. Phys.* **44**, 455 (1927).
5. H. Eyring, M. Polanyi, *Z. Phys. Chem. Abt. B* **12**, 279 (1931).
6. G. R. Fleming, *Chemical Applications of Ultrafast Spectroscopy* (Oxford Univ. Press, Oxford, 1986).
7. P. Kukura *et al.*, *Science* **310**, 1006 (2005).
8. P. Kukura *et al.*, *Annu. Rev. Phys. Chem.* **58**, 461 (2007).

10.1126/science.1166563

BEHAVIOR

A Biolinguistic Agenda

Neurobiology and genetics are helping to generate insights about the evolution of language.

Marc D. Hauser[1] and Thomas Bever[2]

When we transform thoughts into speech, we do something that no other animal ever achieves. Children acquire this ability effortlessly and without being taught, as though discovering how to walk. Damage to specific areas of the brain that are critical to language shows the profound selectivity of cerebral organization, underlining the exquisite biological structure of language and its computational features. Recent advances bring new insights into the neurogenetic basis of language, its development, and evolution, but also reveal deep holes in our understanding.

There are about 7000 living languages spoken in the world today, characterized by both exceptional diversity as well as significant similarities. Despite many controversies in the field, many linguistic scholars generally agree on two points (*1*–*8*). Language as a system of knowledge is based on genetic mechanisms that create the similarities observed across different languages, culturally specific experience that shapes the particular language acquired, and developmental processes that enable the growth and expression of linguistic knowledge. Also, the neural systems that allow us to acquire and process our knowledge of language are separate from those underlying our ability to communicate.

To fulfill a biolinguistic agenda—study of the computational systems inherent to language—we must address the rules and constraints that underlie a mature speaker's knowledge of language; how these rules and constraints are acquired; and whether they are mediated by language-specific mechanisms. We also need to distinguish which rules and constraints are shared with other animals and how they evolved, and to ask how knowledge of language is used in communicative expressions.

There has been little research linking the formal linguistic principles that describe the mature speaker's knowledge of language to the evolutionary, neurobiological, and developmental factors that lead to their instantiation in the adult mind. These principles include computational devices such as hierarchies and dependencies among syntactic categories (e.g., the relationship between determiners such as "the" and "a" followed by nouns), recursive and combinatorial operations, and movement of parts of speech and phrases (e.g., to create a question, many languages move constructions such as "what" or "where" to the front of the sentence). This gap is slowly narrowing, but the separation remains great. It is thus important to clarify the appropriate targets of analysis. In particular, examination of the evolutionary, neurobiological, and developmental aspects of language often focuses narrowly on speech, or in some cases, on the separate issue of communication. Instead, these aspects should be considered in light of the principles discussed, helping to align formal approaches to linguistics with the biological sciences.

Formal approaches to examine linguistic structure are marked by disagreement about the necessary or sufficient computations required to create the expressed languages of the world. Some linguists argue that linguistic form relies on abstract, generative operations that allow phrases and sentences (syntactic structures) to interface with meanings (the semantic system) to create a categorization (lexical terms) in which single words and groups of words convey a specific meaning. Such lexical terms then interface with speech sounds (phonology) to create expressed words in speech or sign. Language has been suggested as an optimal solution to the syntactic-semantics interface, achieved by a small number of computational operations. By comparison, current evolutionary models suggest that the variation in animal body form can be explained by different activation patterns for a few master genes during development. The corresponding idea in linguistics is that the cross-cultural variation in expressed human languages can be explained by a universal set of mental operations, some specific to language, others shared across domains including music, mathematics, and morality (*4*, *9*).

Comparative evolutionary studies suggest that birds, rodents, and primates compute some components of human grammatical

[1]Department of Psychology, Human Evolutionary Biology, Harvard University, Cambridge, MA 02138, USA. [2]Departments of Linguistics, Psychology and Cognitive Science Program University of Arizona, Tuscon, AZ 85721, USA. E-mail: mdh@wjh.harvard.edu

competence, but cannot attach this capacity to their own communication systems (*10*–*12*). For example, birds and primates can compute a first-degree finite state grammar, where elements in a string of sounds have specific orders, each predicted by simple statistical associations. This grammar is one of the simplest within a hierarchy of computational operations of increasing complexity and expressive power (*10*, *13*). The biggest puzzle, however, is why nonhuman animals cannot integrate these computational capacities with their capacity to communicate. So, although songbirds can combine different notes into a variety of songs, they don't integrate this combinatorial capacity with conceptual abilities to create sounds with varied meaning. Understanding what neural connections are absent, or poorly developed, may help account for this evolutionary bottleneck, and explain why human infants readily produce an infinite variety of meaningful expressions.

Damage to Broca's area and Wernicke's area in the human brain results in distinct patterns of language loss, suggesting that properties of the neocortex make language unique to humans. Artificial language studies show that these cortical areas execute the computations that obey language universals (the principles accessed by all languages, such as specific word orders), but other brain areas are also activated by these computations (*14*, *15*). In fact, different cortical areas may compute different kinds of grammars, but such localization does not provide insight into linguistic theories aimed at uncovering principles that guide the mature state of language competence and its acquisition during development.

Does language have its own dedicated brain circuits, or is much or all of this circuitry shared across domains (such as music and language)? For example, language and music rely on hierarchical representations, make use of combinatorial and recursive computations, and generate serially represented structures. But does each domain recruit a general-use ensemble of these processes or does each domain have its own set of processes? Further studies of selective brain damage and brain-imaging experiments should be informative.

Genes associated with particular linguistic deficits can help pinpoint the molecular basis for language, and link issues in evolution with those in development. Yet, we are far from understanding how normal genes are associated with linguistic features. When the gene *FOXP2* was linked to families with a particular language deficit, it seemed that genomics might account for linguistic structure. But the relationship between *FOXP2* and language turns out to be weak. For example, *FOXP2* exists in songbirds and echo-locating bats; although songbirds have richly structured sound systems that might be properly characterized by a finite state grammar, such grammars are not hierarchically structured, lack syntactic categories (e.g., nouns and determiners), and do not productively generate meaningful variation. Further, the disorders associated with *FOXP2* in humans include articulatory disabilities and are not clearly syntactic, semantic, or computational (*16*, *17*). The weak connection between *FOXP2* and these aspects

CREDIT: PETER HOEY

of language should not, however, come as a surprise given that most gene-phenotype relationships involving complex phenotypes (such as language) are weak. Nonetheless, by breaking language down into its component parts and finding potential homologs in other animals (especially those that can be genetically manipulated), we may better understand the evolution, development, and neurobiological breakdown of linguistic function.

Current research on hemispheric lateralization (division of the brain into left and right halves) and language acquisition provides one example of how interdisciplinary work relates to specific theories in linguistics. All right-handed people have strong left-hemisphere lateralization of syntactic function. However, classic investigations of aphasia—the inability to produce or comprehend language—reveal that familially "mixed" right-handers (right-handers with left-handed family members) show more right-hemisphere involvement in language than pure right-handers (*18*, *19*). Thus, in familially mixed right-handers, the right hemisphere's involvement in language may be specific to lexical representations (*20*). Familially mixed right-handers access individual words more readily than global sentence structure, whereas the reverse is true of familially pure right-handers (*21*). Their critical period for language learning is also earlier than that of familially pure right-handers (*22*), which suggests that mixed right-handers are more likely to base their language learning on the acquisition of words as opposed to syntactic structure. These findings are supported by brain-imaging research showing that familially pure right-handers have left-hemisphere activation during lexical access, whereas familially mixed right-handers show more bilateral hemisphere activation (*23*). At the same time, all subjects show left-hemisphere activation for syntactic processes. This confirms the basic hypothesis that mixed right-handers have more distributed representations of lexical knowledge.

What are the implications of such population-level differences in lexical use, access, and representation for linguistic theory? In recent decades, syntacticians have struggled with the role of the lexicon in syntactic architectures. Proposals range from the traditional view that the lexicon is distinct from the computations of syntax, to the view that syntax itself is driven by lexical structures. The observed variability in how the lexicon is accessed and represented suggests that it is indeed a biologically separable component of linguistic knowledge.

Brain imaging, genomics, and new methods for comparative studies have provided the means for better understanding the shared and uniquely human components of language. As some linguists argue, the variation in linguistic form among the world's languages may be as superficial as the variation in animal body forms. The superficiality arises, in each case, because of universal computations that provide the necessary suite of developmental programs to generate the variation. As the biolinguistic agenda advances, however, new generations of linguists will be required to translate their formalisms into testable experiments by biologists and psychologists. For example, language deploys recursive operations and generates hierarchical representations with specific configurations. It is not yet clear how to design experiments to test whether nonlinguistic organisms can acquire these representations, or what factors limit either their acquisition or implementation into communicative expression. Conversely, psychologists and biologists will need to be sensitive to the limitations of their methods and the extent to which they can test linguistic theories. Thus, neuropsychological studies showing deficits in language need

to be accompanied by comparable tests in nonlinguistic domains to show that they are language-specific deficits. And studies using brain imaging must acknowledge that localization of function does not provide explanatory power for the linguist attempting to uncover principles underlying the speaker's knowledge of language. These cautions aside, the biolinguistic approach is clearly benefiting from modern technologies to advance our knowledge of what language is, how it is represented, and where it came from.

References

1. M. A. Arbib, *Behav. Brain Sci.* **28**, 105 (2005).
2. E. Bates, *Discuss. Neurosci.* **10**, 136 (1994).
3. T. G. Bever, in *Cognition and Language Development*, R. Hayes, Ed. (Wiley, New York, 1970), pp. 277–360.
4. N. Chomsky, *Linguist. Inq.* **36**, 1 (2005).
5. T. W. Deacon, *The Symbolic Species: The Coevolution of Language and the Brain* (Norton, New York, 1997).
6. R. Jackendoff, *Foundations of Language* (Oxford Univ. Press, New York, 2002).
7. E. H. Lennenberg, *Biological Foundations of Language* (Wiley, New York, 1967).
8. S. Pinker, *Language Learnability and Language Development* (Harvard Univ. Press, Cambridge, MA, 1984).
9. C. Boeckx, M. Piatelli-Palmerini, *Linguist. Rev.* **22**, 447 (2005).
10. W. T. Fitch, M. D. Hauser, *Science* **303**, 377 (2004).
11. T. Q. Gentner, K. M. Fenn, D. Margoliash, H. C. Nusbaum, *Nature* **440**, 1204 (2006).
12. R. A. Murphy, E. Mondragon, V. A. Murphy, *Science* **319**, 1849 (2008).
13. N. Chomsky, *Syntactic Structures* (Mouton, the Hague, 1957).
14. A. Friederici *et al.Proc. Nat. Acad. Sci.* **103**, 2458 (2006).
15. M. Musso *et al.*, *Nat. Neurosci.* **6**, 774 (2003).
16. W. Enard *et al.*, *Nature* **418**, 869 (2002).
17. S. Haesler *et al.*, *J. Neurosci.* **24**, 3164 (2004).
18. A. R. Luria, *Traumatic Aphasia* (Mouton, the Hague, 1969).
19. J. T. Hutton, N. Arsenina, B. Kotik, A. R. Luria, *Cortex* **13**, 195 (1977).
20. T. G. Bever, C. Carrithers, W. Coward, D. J. Townsend, in *From Neurons to Reading*, A. Galaburda, Ed. (MIT Press, Cambridge, MA, 1989).
21. D. J. Townsend, C. Carrithers, T. G. Bever, *Brain Lang.* **78**, 308 (2001).
22. D. S. Ross, T. G. Bever, *Brain Lang.* **89**, 115 (2004).
23. S. Chan, thesis, University of Arizona (2007).

10.1126/science.1167437

BIOCHEMISTRY

RT Slides Home...

To access its target sites, HIV reverse transcriptase slides and flips on nucleic acid substrates.

Stefan G. Sarafianos[1] and Eddy Arnold[2]

For HIV to replicate inside human cells, it must convert its single-stranded RNA genome into double-stranded DNA that can be integrated into the host genome (*1*). This formidable task is achieved by HIV reverse transcriptase (RT), a multifunctional enzyme that has RNA-dependent and DNA-dependent DNA polymerase activities to synthesize minus and plus DNA strands, ribonuclease H (RNase H) activity to degrade the RNA strand of the RNA-DNA replication intermediate, a strand displacement activity to remove the remaining RNA and DNA fragments to allow synthesis of the plus DNA strand, and a strand transfer activity to move newly synthesized DNA within or between templates. Although 20 years of crystallographic and biochemical studies have illuminated the molecular details of the chemistry of DNA synthesis, there have been relatively few insights into how RT finds the end of the nucleic acid substrate where it begins DNA synthesis, how it displaces nucleic acid fragments, or where and how it executes masterful leaps when transferring DNA between templates. On page 1092 of this issue, Liu *et al.* (*2*) describe elegant single-molecule fluorescence resonance energy transfer (FRET) experiments that provide a view of RT at work. They show that RT has a remarkable ability to slide on nucleic acid duplexes, rapidly shuttling between the two ends and flipping into the polymerase-competent binding mode when needed.

Important structural features of RT (*3*, *4*) and its molecular interactions with substrates and inhibitors have been elucidated through extensive crystallographic studies (*4*–*7*). HIV RT is an asymmetric heterodimer composed of p66 and p51 subunits that have identical amino termini. The p66 subunit has enzymatic activity, containing the spatially distinct polymerase and RNase H active sites, whereas the smaller p51 subunit plays a structural role. The p66 polymerase domain comprises four subdomains: fingers, palm, thumb, and connection. Although p51 folds into the same subdomains as the polymerase domain of p66, the positions of the subdomains relative to each other are different in p66 and p51.

In this study, Liu *et al.* use a single-molecule FRET assay to measure the position and orientation of RT relative to its nucleic acid substrate. They immobilized nucleic acid labeled at one end of the template or primer strand with the FRET acceptor fluorophore, Cy5, and immersed it in a solution containing RT molecules labeled with a FRET donor dye, Cy3, attached either at the RNase H domain or at the fingers domain of the p66 subunit. By monitoring the FRET efficiency, they were able to determine the enzyme's position on the nucleic acid substrate during each binding event. The same team (groups of Zhuang and Le Grice) recently used this approach to show that RT can rapidly switch between two orientations when it binds duplexes containing the unique polypurine RNA sequences that are primers for plus-strand synthesis (*8*). Now they show that the enzyme can slide between opposite termini on long duplexes and that the flipping and sliding kinetics are altered in the presence of nevirapine, a non-nucleoside inhibitor of HIV RT (NNRTI).

Here, the authors pose the question: How does RT efficiently locate the 3′ terminus of nascent DNA on a long duplex substrate so that it can extend it? This question is particularly important because HIV RT has relatively low processivity and must frequently locate the polymerization site after dissociation. Also, RT cleaves RNA-DNA hybrids at many different sites, and it is not well understood how it accesses these sites (*9*, *10*).

In answer to these questions, Liu *et al.* initially showed that RT binds an oligonucleotide that is the same size as its nucleic acid binding cleft (19 base pairs) only in the configuration that places its polymerase site at the 3′ end of the primer ("front-end" binding). However, when RT binds longer RNA-DNA (or DNA-DNA) substrates (38 or 56 base pairs), there is an equilibrium between front-end and back-end binding that favors front-end binding (see the figure). Therefore, the enzyme can stably bind either to the front end of the hybrid, poised for DNA extension, or to the back end, placing the RNase H domain close to the 3′ of the RNA (or DNA) template.

By following changes in FRET over time, Liu *et al.* were able to detect repeated transitions between front- and back-end bound states within a single binding event, suggesting that shuttling can occur between these

[1]Christopher S. Bond Life Sciences Center, Department of Molecular Microbiology and Immunology, University of Missouri, 1201 Rollins Street, Columbia, MO 65211, USA. [2]Center for Advanced Biotechnology and Medicine, Department of Chemistry and Chemical Biology, Rutgers University, 679 Hoes Lane, Piscataway, NJ 08854, USA. E-mail: sarafianoss@missouri.edu; arnold@cabm.rutgers.edu

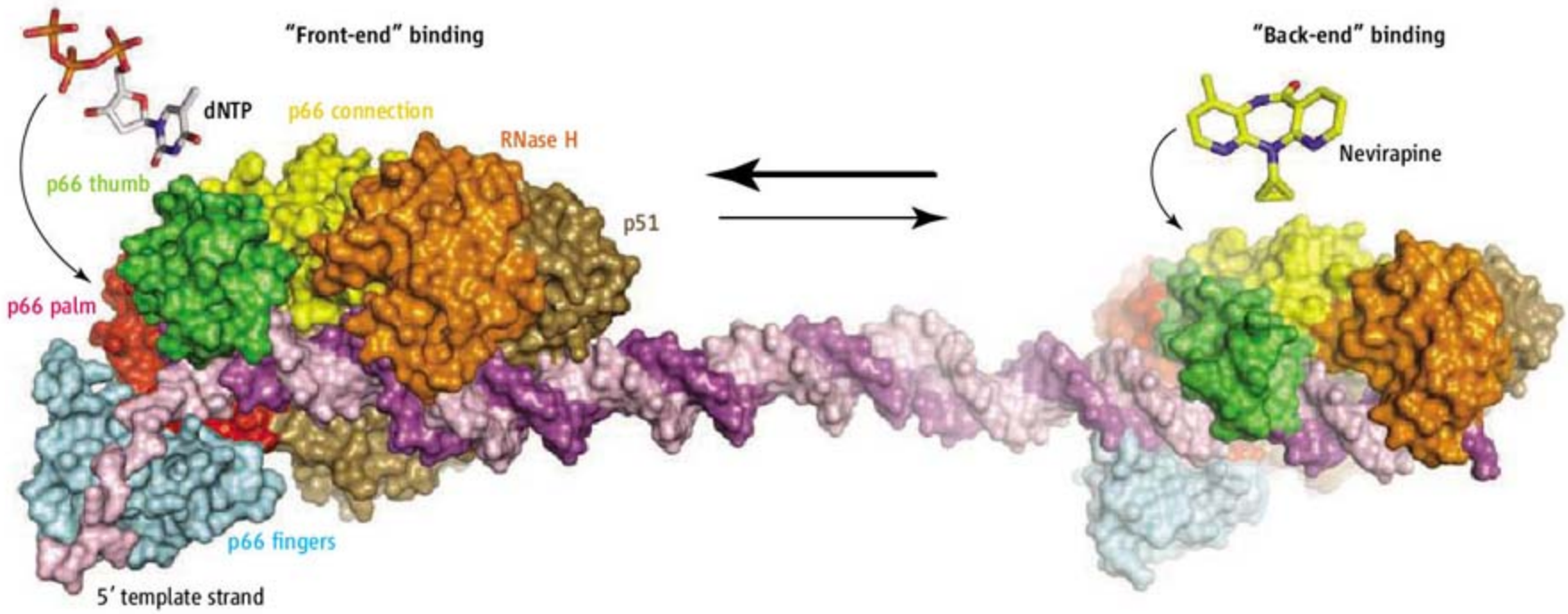

RT slides on a nucleic acid substrate without dissociating. Binding at the 3′ primer end (front-end binding) is favored over binding at the other end. However, in the presence of deoxyribonucleotide triphosphate (dNTP), RT becomes locked in a front-end binding conformation, whereas in the presence of nevirapine it shifts toward back-end binding. p66 (fingers in cyan, palm in red, thumb in green, connection in yellow, RNase H in orange) and p51 (brown) are the large and small subunits of the RT heterodimer bound to an RNA-DNA template (pink) primer (magenta).

states without dissociation (see the figure). The shuttling is a thermally driven diffusion process that does not require energy from nucleotide hydrolysis. RT can cleave RNA at multiple positions within a DNA-RNA hybrid (*9*), and the sliding function of RT may provide a mechanism by which the enzyme can rapidly access these cleavage sites.

The authors also identified factors that modulated the ability of the enzyme to slide on the nucleic acid substrate. A cognate nucleotide favors front-end binding in the polymerization mode (see the figure); in contrast, the NNRTI nevirapine destabilized the polymerization binding mode, presumably because it binds at the base of the p66 thumb subdomain of RT and affects its ability to grasp the nucleic acid. On the basis of these results, Liu *et al.* conclude that for RT to escape from the polymerization mode, a relaxation of the fingers-thumb grip is likely to be required.

Other nucleic acid binding proteins are also thought to use a one-dimensional sliding diffusion along the nucleic acid to locate their targets (references 38 to 42 in Liu *et al.*). However, RT may add a twist to this mechanism. A tantalizing finding in the Liu *et al.* paper is that RT may bind the "wrong" way on the nucleic acid and still find its way to the 3′-OH of the nascent DNA, where it flips into the polymerization-competent orientation. This surprising trick may be used by RT to increase its efficiency of binding in a polymerization-competent mode.

This unexpected property challenges our assumptions of RT gripping the nucleic acid in a single defined way, and highlights a remarkable flexibility that may be the hallmark of multifunctional enzymes. Nonetheless, it is consistent with the ability of the RT fingers and thumb subdomains to undergo large conformational changes during the polymerization reaction. This finding may also shed light on how the enzyme is able to jump from one RNA genome to another during reverse transcription, resulting in increased recombination rates and evolutionarily important genome diversity. Interestingly, unlike RT, viral RNA-dependent RNA polymerases with related architecture for polymerase catalysis appear to form structures reminiscent of tightly closed rings (*11*) that ensure unidirectional synthesis (either replication or transcription) after initiation.

Dissociated RT does not simply have to relocate the polymerization site during strand displacement synthesis. It may have to locate disrupted polymerization sites where the primer terminus has been displaced from the template by the competing nontemplate strand. The authors' data suggest that sliding allows RT to efficiently access the disrupted polymerization site and assist primer-template annealing, thereby facilitating RNA strand displacement synthesis.

In another striking experiment, Liu *et al.* used the single-molecule FRET method to observe a single RT molecule carrying out processive DNA synthesis or pausing in real time, as indicated by plateaus in the single-molecule FRET. This remarkable technical achievement bodes well for future studies that could focus on the mechanisms by which RT translocates or pauses on nucleic acid substrates.

The Liu *et al.* report vividly illustrates that RT has a remarkable dynamic flexibility that contributes to more efficient replication by allowing it to bind nucleic acids in multiple conformations and to slide over long distances toward the ends of the nucleic acid duplexes. Future challenges will be to enhance the complexity of the system by including components that are known to affect the efficiency and outcome of the polymerization reaction. For example, how might the sliding and flipping functions be affected on genomic RNA with considerable secondary structure? Also, what is the mechanism by which the nucleocapsid protein affects the strand transfer and processivity functions of RT (*12*, *13*)?

References

1. J. M. Coffin, S. H. Hughes, H. E. Varmus, *Retroviruses* (Cold Spring Harbor Laboratory Press, Cold Spring Harbor, NY, 1997).
2. S. Liu, E. A. Abbondanzieri, J. W. Rausch, S. F. J. Le Grice, X. Zhuang, *Science* **322**, 1092 (2008).
3. L. A. Kohlstaedt, J. Wang, J. M. Friedman, P. A. Rice, T. A. Steitz, *Science* **256**, 1783 (1992).
4. A. Jacobo-Molina *et al.*, *Proc. Natl. Acad. Sci. U.S.A.* **90**, 6320 (1993).
5. J. Ren *et al.*, *Nat. Struct. Biol.* **2**, 293 (1995).
6. H. Huang, R. Chopra, G. L. Verdine, S. C. Harrison, *Science* **282**, 1669 (1998).
7. S. G. Sarafianos *et al.*, *EMBO J.* **20**, 1449 (2001).
8. E. A. Abbondanzieri *et al.*, *Nature* **453**, 184 (2008).
9. J. J. DeStefano, L. M. Mallaber, P. J. Fay, R. A. Bambara, *Nucleic Acids Res.* **21**, 4330 (1993).
10. M. Wisniewski, M. Balakrishnan, C. Palaniappan, P. J. Fay, R. A. Bambara, *J. Biol. Chem.* **275**, 37664 (2000).
11. Y. Tao, D. L. Farsetta, M. L. Nibert, S. C. Harrison, *Cell* **111**, 733 (2002).
12. J. C. You, C. S. McHenry, *J. Biol. Chem.* **269**, 31491 (1993).
13. L. Rodriguez-Rodriguez, Z. Tsuchihashi, G. M. Fuentes, R. M. Bambara, P. J. Fay, *J. Biol. Chem.* **270**, 15005 (1995).

10.1126/science.1167454

CLIMATE CHANGE

Understanding Glacier Flow in Changing Times

Subannual lurches of the Greenland and Antarctic ice sheets may reduce uncertainties about climate change effects on sea-level rise.

Richard B. Alley,[1] Mark Fahnestock,[2] Ian Joughin[3]

Unexpected accelerations in outlet glaciers of the Greenland and Antarctic ice sheets in the last decade, in response to processes not fully understood, prompted the Intergovernmental Panel on Climate Change (IPCC) Fourth Assessment to conclude that poorly characterized uncertainties prevented a best estimate or upper bound on sea-level rise. These changes in ice sheet outlet glaciers come at a time when smaller glaciers and ice caps are wasting quickly as well. The focus of present glacier research must be the rapid reduction of the uncertainty identified by the IPCC. Rapid progress will require identification of the most relevant of the recent changes, effective moves toward understanding the controlling physics, and careful consideration of the differing time scales involved. We briefly review recent changes with a view toward an effective path forward.

About 6 years ago, Zwally *et al.* discovered that lubricating surface meltwater can reach the base of the Greenland Ice Sheet, thereby speeding up summer ice flow (*1*). Subsequent work confirms the broad picture of seasonal lubrication (*2*) but shows that annual motion is enhanced only by 10 to 20% (*3*). More important, the fast outlet glaciers responsible for most of the ice discharge to the ocean are relatively insensitive to summer melt, making it unlikely that enhanced seasonal lubrication will destabilize the ice sheet (*2*).

Meltwater drainage to the bed can play a second and possibly more important role, however, speeding ice flow by delivering heat rapidly to the bed. The water in surface lakes (see the figure) can wedge open crevasses, fracturing through to the bed catastrophically (*4*). Were this phenomenon to spread inland in a warming world, it would deliver sufficient heat to thaw areas where the bed is currently frozen (*5*). In this event, twofold accelerations would not be surprising, with the slight chance of an order-of-magnitude or more locally if extensive regions with soft sediments were to thaw (*6*). Some issues remain: Reliable mapping of the basal characteristics of regions now frozen but that might thaw is unavailable, and our present understanding is not sufficient to tell us whether inland migration of melting will be accompanied by the changes in ice flow required to open cracks beneath any new lakes.

Lakes exist not only on top of but also beneath the ice. Increasingly seen to be widespread and dynamic, these subglacial lakes occur at and may be linked to the upglacier limit of rapid ice flow (*7*). However, release of stored lake water in outburst floods (*8*) does not seem to have major ice-flow effects. It is even possible that an ice sheet with more subglacial lakes will be less variable, because the lakes focus water drainage in space and time and thus reduce lubrication overall.

Far more ominous for future sea levels are the changes that originate where ice meets ocean. Ice shelves, the floating-but-still-attached parts of the ice sheets extending over the ocean, restrain the nonfloating ice through friction with local bedrock highs or with fjord walls. Because ice shelves are near sea level and in contact with the ocean, they are the elements of the coupled sheet-shelf system that are most susceptible to warming. Extensive surface melting can fill surface crevasses and destroy an ice shelf through the same fracture process that allows surface lakes to drain to the bed (*9*). Furthermore, even small changes in water temperature below the ice shelf can speed basal melting by roughly 10 meters per year for each 1°C warming (*10*).

Such wasting of shelves has no direct effect on sea level, but the loss of restraint and associated acceleration of inland flow to the ocean has triggered doublings of flow speed, with one change reaching eightfold (*11*). Large diurnal changes in flow speed of Antarctic ice streams feeding ice shelves occur in response to the small changes in loading at the ends caused by the tides (*12*), showing that these ice streams will respond rapidly if the buttressing from their ice shelves is reduced. Ice shelves are far less prevalent in Greenland than in Antarctica, but loss of floating and grounded ice at marine-terminating outlet glaciers has had similarly large effects (*13*). Present seasonal acceleration in the flow speed of Jakobshavn Glacier in Greenland begins in response to loss of sea ice damming the fjord. This commences well before the springtime onset of surface melt (*14*).

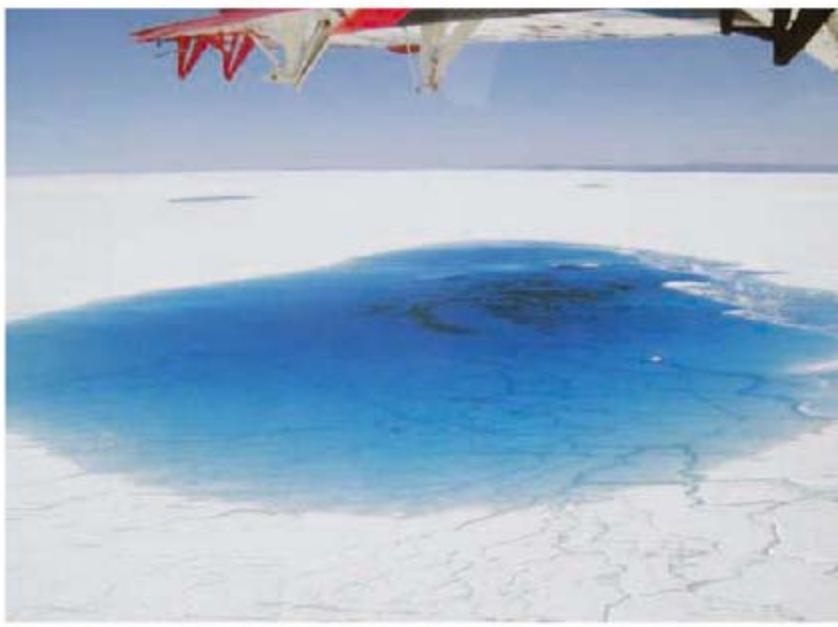

Lakes on the western flank of the Greenland Ice Sheet. The nearest lake is roughly 1500 m across and 10 m deep. Meltwater from these lakes can drain catastrophically into the ice sheet, causing brief but strong local disturbance of the ice flow. More important, these drainage events establish a meltwater pathway from surface to bed. Inland migration of this phenomenon might thaw now-frozen regions of the ice-sheet bed and speed up flow. The wing of a De Havilland Twin Otter occupies the top of the frame.

CREDIT: IAN JOUGHIN/UNIVERSITY OF WASHINGTON

In the absence of validated models incorporating these processes, scientists have turned to a range of ice-flow scaling exercises and back-of-the-envelope estimates to constrain estimates of future ice-sheet contributions to sea-level change (see supporting online material). Although these estimates are instructive and useful, there is a lack of strong convergence among them, and a wide range of possible answers remains.

Progress toward more rigorously quantitative estimates will not be easy. When each major new project turns up something unexpected, we can be confident that the field is undersampled. For decades, the major atmo-

[1]Department of Geosciences and Earth and Environmental Systems Institute, Pennsylvania State University, University Park, PA 16802, USA. E-mail rba6@psu.edu [2]Institute for the Study of Earth, Oceans, and Space, University of New Hampshire, Durham, NH 03824, USA. [3]Polar Science Center, Applied Physics Laboratory, University of Washington, Seattle, WA 98105–6698, USA.

sphere-ocean general-circulation modeling groups have assumed that ice sheets are static, white mountain ranges; reversing this approach by having such groups develop sophisticated treatments of ice sheets would unleash great talent on this crucial problem. Such a modeling effort, however, must be coordinated tightly with remote-sensing, field- and laboratory-based efforts to understand the processes that control ice flow.

Perhaps the key uncertainty remains the interaction between the ice and its underlying bed, which controls how basal velocity will change as ice-sheet stresses evolve. Geophysical exploration is essential but, realistically, cannot sample everything. Inversions from remotely sensed data provide modern snapshots (*15*) but do not elucidate the dependence of basal velocity on changing stress. If we wait for the ice sheets to evolve through a wide enough range of stresses, then we or some future generation of glaciologists will retrodict changes rather than predict them usefully.

Fortunately, the lake drainages, calving events, tidal responses, and other recently observed phenomena discussed above are exciting the ice sheet, providing short-period samples of a wide range of stress and lubrication states and the associated velocity response necessary to characterize the system. Such short-period changes, however, are so fast that they have been difficult to observe fully and may involve elastic responses that are not captured by comprehensive ice-flow models. A more holistic approach that uses appropriately designed experiments that assimilate ground-based and remotely sensed data into improved models may provide the improved understanding needed to constrain future sea-level changes.

Although crucial, such experiments are increasingly difficult, as field efforts are eliminated or delayed in the face of rising fuel costs (*16*). The U.S. National Aeronautics and Space Administration's Decadal Survey missions addressing ice [the Ice, Cloud, and land Elevation Satellite II (ICESAT-II) and the Deformation, Ecosystem Structure, and Dynamics of Ice (DESDynI) mission] are a number of years from providing data to replace those endangered by failing satellites and access limitations. In the interim, this gap could be partly closed through closer coordination and improved data distribution among the various space agencies that operate the international constellation of remote-sensing spacecraft.

For a student of ice flow, these are exciting times, with the pace of discovery seemingly accelerating. For a student of policy, the possibility looms of a fifth IPCC assessment lacking projections of sea-level rise sufficiently constrained for effective policy design. Wise choices may yet beat this unpleasant outcome. A coupled observation and modeling approach that lets the ice sheets tell us the answer may be the quickest path.

References

1. H. J. Zwally *et al.*, *Science* **297**, 218 (2002).
2. I. Joughin *et al.*, *Science* **320**, 781 (2008).
3. R. S. W. van de Wal *et al.*, *Science* **321**, 111 (2008).
4. S. B. Das *et al.*, *Science* **320**, 778 (2008).
5. B. R. Parizek, R. B. Alley, *Quat. Sci. Rev.* **23**, 1013 (2004).
6. R. B. Alley, I. M. Whillans, *Science* **254**, 959 (1991).
7. R. E. Bell *et al.*, *Nature* **445**, 904 (2007).
8. H. A. Fricker *et al.*, *Science* **315**, 1544 (2007).
9. T. A. Scambos *et al.*, *J. Glaciol.* **46**, 516 (2000).
10. E. Rignot, S. S. Jacobs, *Science* **296**, 2020 (2002).
11. E. Rignot *et al.*, *Geophys. Res. Lett.* **31**, L18401 (2004).
12. S. Anandakrishnan *et al.*, *Geophys. Res. Lett.* **30**, 1361 (2003).
13. I. M. Howat *et al.*, *Science* **315**, 1559 (2007).
14. I. Joughin *et al.*, *J. Geophys. Res.* **113**, F01004 (2008).
15. I. Joughin *et al.*, *J. Geophys. Res.* **109**, B09405 (2004).
16. E. Kintisch, *Science* **321**, 1142 (2008).

Supporting Online Material

www.sciencemag.org/cgi/content/full/322/5904/1061/DC1
SOM Text
References

10.1126/science.1166366

MICROBIOLOGY

A Protein Pupylation Paradigm

Tagging proteins with ubiquitin molecules so that they will be degraded in the proteasome is not a mechanism unique to eukaryotes.

Sohini Mukherjee[1] and Kim Orth[2]

Tuberculosis, a devastating infectious disease caused by *Mycobacterium tuberculosis* (*Mtb*), is a global health threat that presently afflicts one-third of the world's population. The culprit bacterium is an obligate and persistent pathogen that maintains viability, in a latent state, within phagocytes—cells that ingest foreign materials and microorganisms—that reside in the lungs of humans. Treating tuberculosis requires prolonged antibiotic therapy that can result in multidrug-resistant *Mtb* strains. Because the bacterium is highly infectious, grows extremely slowly, and is difficult to manipulate genetically, the discovery of new drugs to combat *Mtb* infection is challenging. Thus, identifying *Mtb* components as potential drug targets is one of the key approaches to developing new tuberculosis therapies. On page 1104 of this issue, Pearce *et al.* (*1*) report the discovery of a protein (Pup) in *Mtb* that modifies other bacterial proteins to target them for degradation. The process is similar to that in eukaryotes, in which the protein ubiquitin modifies proteins and targets them for proteolysis (see the figure). The discovery of this process in prokaryotes opens the door to further characterizing a protein regulatory mechanism that could be targeted by pathogen-specific drugs.

The proteasome is an adenosine 5′-triphosphate (ATP)–dependent protein degradation complex present in eukaryotes, as well as in several archaebacterial and eubacterial species, including *Mtb* (*2*). The *Mtb* proteasome system, however, is not well characterized, and its functions remain elusive. Nitric oxide, an important signaling molecule, slows the growth of *Mtb*; genetic inactivation of an enzyme that produces nitric oxide (inducible nitric oxide synthase) increases the susceptibility of mice to *Mtb* infection (*3*). Two *Mtb* proteins, *Mycobacterium* proteasomal adenosine triphosphatase (ATPase) and proteasome accessory factor A, were identified in screens for factors that increase susceptibility of the bacterium to the lethal effects of nitric oxide. *Mycobacterium* proteasomal ATPase forms hexamers and exhibits ATPase activity similar to that of the eukaryotic ATPases involved in proteasome function (*3*). ATPase activity is required for the recognition, unfolding, and translocation of substrates into the proteasomal core in eukaryotes. *Mtb* bacteria that are resistant to nitric oxide, and consequently exhibit increased virulence in mice, require proteasomal activity, thereby linking protein degradation to pathogenesis. Interestingly, autophagy, another form of protein degradation in eukaryotes, is linked to a mechanism that inhibits the survival of *Mtb* within host cells independent of nitric oxide (*4*).

[1]Department of Immunology, University of Texas Southwestern Medical School, Dallas, TX 75230, USA. [2]Department of Molecular Biology, University of Texas Southwestern Medical School, Dallas, TX 75230, USA. E-mail: kim.orth@utsouthwestern.edu

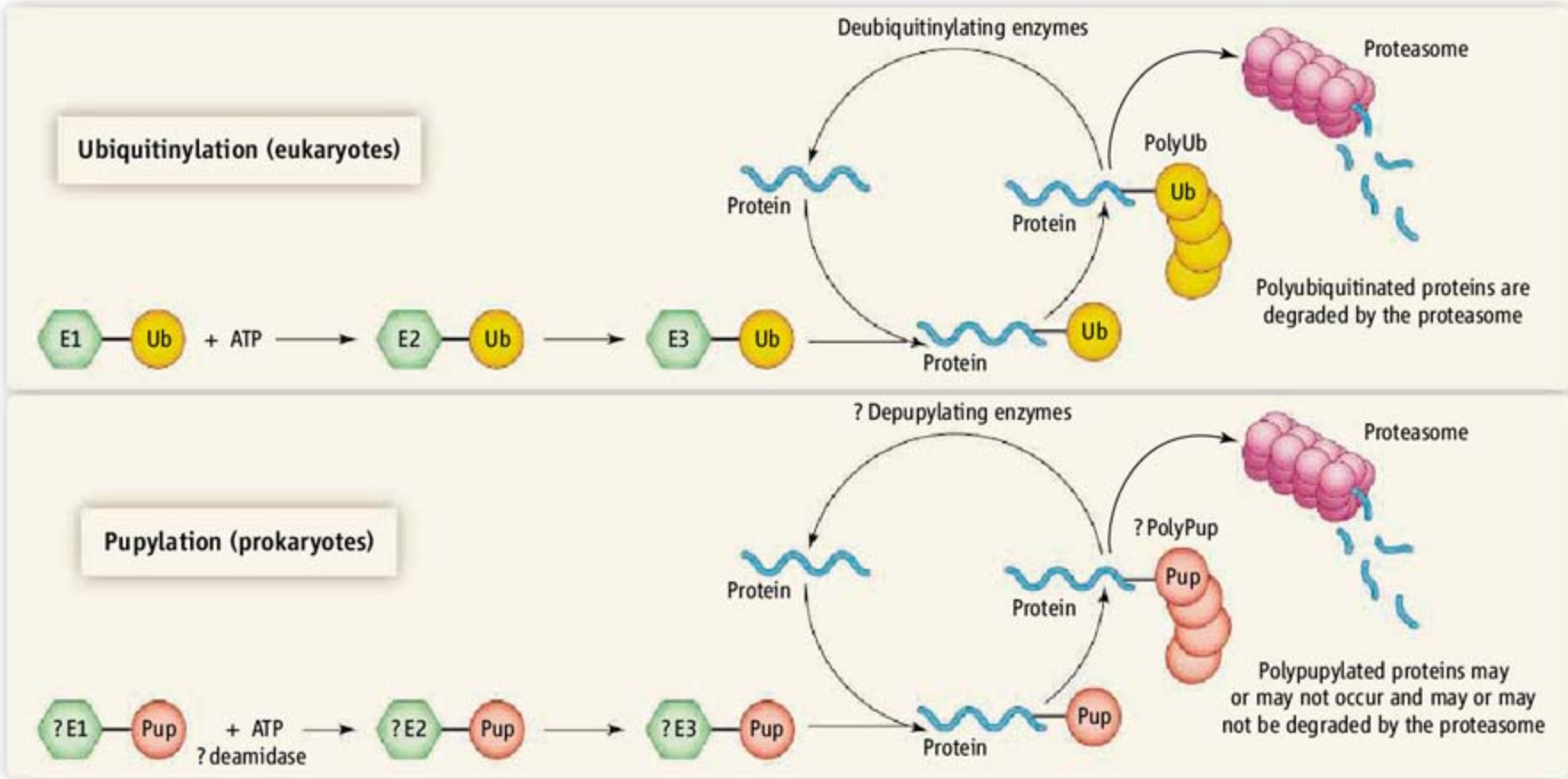

Degradation parallels. Proteins in eukaryotes and prokaryotes are similarly modified by the small proteins ubiquitin (Ub) and Pup, respectively, targeting them for destruction by the proteasome. However, the specific mechanisms are likely to be different.

To understand how proteins are targeted for degradation in *Mtb*, Pearce *et al.* successfully defined the proteasome system in the bacterium, identified the first prokaryotic ubiquitin-like protein, and discovered a mechanism for activating and conjugating this protein to its substrates based on a unique chemistry. The authors identified Pup, a 6.9-kD protein, while searching for potential binding partners for *Mycobacterium* proteasomal ATPase. The carboxyl-terminal sequence (Gln-Lys-Gly-Gly-Gln) of Pup is very similar to the motif (X-X-Gly-Gly, where X is any amino acid) found at the end of most ubiquitin-like proteins. The carboxyl terminus of ubiquitin-like proteins is processed to expose the Gly-Gly portion of the motif, which prepares it for conjugation to substrates. The carboxyl-terminal glycine can covalently link, via an isopetide bond, to a lysine in the target protein (*5*).

Pearce *et al.* demonstrate that Pup must become activated as well, but the enzymatic activity responsible for its conversion to an active form remains to be identified. As well, enzymes that conjugate activated Pup to substrates—similar to the ligases (E1, E2, and E3) that conjugate ubiquitin to substrates—have not been identified either. By contrast, homologs of the proteasome core and associated ATPases have been identified in *Mtb* (and in other bacteria). This suggests that the mechanism of attachment of Pup to substrates is different from that of eukaryotes, or that the *Mtb* enzymes involved share little amino acid similarity with their eukaryotic counterparts. Undetectable amounts of Pup-conjugated proteasome substrates in strains of *Mtb* that lack functional proteasome accessory factor A hint at the involvement of this factor in the modification process.

Pearce *et al.* used mass spectrometry to characterize Pup activation and its conjugation to a *Mtb* proteasome substrate. The authors demonstrate the formation of an isopeptide bond between a lysine residue on the substrate and the carboxyl terminus of Pup—an event called "pupylation." Strikingly, although Pup has a penultimate Gly-Gly motif, the linkage giving rise to pupylation is atypical in that Pup is attached to a substrate via a glutamate within a Gln-Lys-Gly-Gly-Glu motif. Clearly, this mechanism is distinct from ubiquitination in at least two ways (*6*). Pup protein is not proteolytically activated to reveal a carboxyl-terminal Gly-Gly motif that is used in the subsequent conjugation step. Also, the amino acid at the carboxyl terminus of Pup that is conjugated to the target protein is glutamate, not glutamine. This supports the authors' hypothesis that Pup is deamidated before or during conjugation to substrates. Similar to ubiquitin, the activated form of Pup is covalently attached to a specific lysine residue of a proteasome substrate. Thus, although pupylation differs from ubiquitination in terms of the mechanism of conjugation, it appears to affect the demise of target proteins through a similar process of proteasome-mediated degradation.

Besides protein degradation, pupylation may have other functional consequences for proteins, ranging from subcellular sorting to secretion. For example, unlike eukaryotes, bacteria do not have subcellular organelles or a nuclear membrane, yet certain proteins need to be properly localized for bacteria to be viable and proliferate. Like eukaryotic ubiquitination, NEDDylation, or SUMOylation, the discovery of this prokaryotic posttranslational protein modification raises many questions about how proteins are targeted for pupylation. Like ubiquitin, does Pup get removed from proteins and recycled? Also, the enzymes that use this unique chemistry for conjugation may represent candidates for drug targeting. Most importantly, the study by Pearce *et al.* presents an exciting new paradigm for protein regulation by bacteria.

References and Notes

1. M. J. Pearce, J. Mintseris, J. Ferreyra, S. P. Gygi, K. H. Darwin, *Science* **322**, 1104 (2008); published online 2 October 2008 (10.1126/science.1163885).
2. A. Lupas, P. Zwickl, W. Baumeister, *Trends Biochem. Sci.* **19**, 533 (1994).
3. M. J. Pearce *et al.*, *EMBO J.* **25**, 5423 (2006).
4. M. G. Gutierrez *et al.*, *Cell* **119**, 753 (2004).
5. E. S. Johnson, *Annu. Rev. Biochem.* **73**, 355 (2004).
6. K. H. Ventii, K. D. Wilkinson, *Biochem. J.* **414**, 161 (2008).
7. K.O. is an Arnold and Mabel Beckman Young Investigator, a Burroughs Wellcome Investigator, and a W. W. Caruth Jr. Scholar. S.M. is a Helen Hay Whitney Postdoctoral Fellow.

10.1126/science.1166485

Physiographic Control on the Development of *Spartina* Marshes

Gerardo Fragoso[1]* and Tom Spencer[2]

Spartina grasses, which form extensive marshes throughout the temperate world and often constitute the lowest vascular cover relative to sea level, have been prominent in the development of current ideas on coastal wetland development and response to physiographic change. Over the past five decades, a substantial body of research has indicated that *Spartina* production is primarily regulated by submergence and the resulting edaphic conditions (*1*–*3*). The physical sedimentary environment is in turn considered to affect production through its effect on marsh-surface elevation relative to sea level. However, our results working with *Spartina anglica* (*2*) show that production and marsh perennation are controlled by variation in surface level relative to the plant's meristematic base and are not hindered by prolonged submergence (*4*). Experimental ground-level displacement above the original marsh surface resulted in displacement of *Spartina*'s basal meristematic zone to a higher base (Fig. 1) consistently located about 2 cm below the new surface, from which a new clonal cohort emerged, leaving below the old base with its earlier, senescent cohort.

Although accretion is known to foster production, the effect has been attributed to the ameliorating effects of increased elevation on the putative negative impact of increased submergence, from sea-level rise, on plant vigor (*5*). However, orthogonal disaggregation of surface-level displacement and submergence conditions shows that, after taking into account the effect of submergence, growth was significantly greater in plants subject to upward surface-level displacement of only 2.5 cm than in plants in control treatments, whereas plant growth after a reduction in surface level of 1.0 cm was significantly lower than that in controls. In turn, after the effect of surface-level changes was taken into account, plants under continuous submergence showed significantly greater growth than those under intermittent inundation, whereas no significant difference in shoot growth occurred under continuous submergence whether the growing medium was aerated or stagnant. Although *Spartina* establishes perennial marshes, perennation depends chiefly on vegetative reproduction of individual clonal modules, which have a life span of 1 or 2 years (*2*). We suggest that basal-meristem displacement provides the basis of marsh perennating strategy because an accretionary environment enables regular meristematic, and therefore vegetative, renewal. In turn, with a location only about 2 cm below ground surface required for basal-meristem establishment, even a small degree of erosion can expose the basal zone, hindering production. We thus suggest that production of clonal cohorts from the same, aging base in poor sedimentary environments leads to marsh senescence.

The applicability of our findings to other marsh plants remains to be tested. However, the morphological and paradigmatic parallels between *S. anglica*, its genetic parents, and other low-lying rhizomatous halophytes suggest that this mechanism may be involved more generally in the process of marsh development. Analysis of *Spartina* marshes has shown that marsh distribution is not related to sea level, although confirming that primary forcing is exerted by a then-undetermined factor regulated by tidal range (*2*, *6*). Our findings indicate that the sedimentary environment, which is tidally regulated, directly controls production and vegetative renewal, whereas prolonged submergence does not hinder growth of vegetative modules that emerge from new basal meristems. Edaphic products of submergence, such as interstitial sulfide, apparently deleterious in hydroponic conditions, have been found to be innocuous or even beneficial in solid substrate (*7*). Moreover, susceptibility to hypoxic conditions has been observed when experimental subjects are short forms (*8*), which commonly grow in poor accretionary environments and are therefore likely to originate from aging meristematic bases. Sedimentation and submergence often operate collinearly in the field: Stagnant areas are often sediment-starved, and sedimentary-active areas are often well drained. Thus, correlational observations may attribute the effects of sedimentary conditions on production to submergence unless both variables are experimentally disaggregated. When measured across several marshes, data on production and on sulfide distributions show no consistent relationship, with greater differences occurring between, rather than within, marshes (*7*). Our findings may also provide an explanation for the phenomenon of *Spartina* die-back, the causes for which have remained elusive for more than half a century (*2*, *3*, *7*). Although marsh production is known to be affected by a wide variety of both bottom-up and top-down factors, current theory of marsh ecology holds that stress from submergence is a major control. Our results suggest that plant responses to changes in sedimentary conditions determine marsh development and survival in the short term, independently of long-term changes in relative sea level.

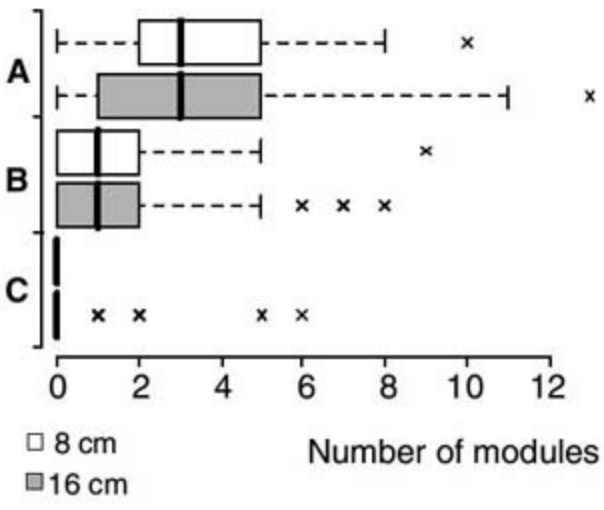

Fig. 1. Number of clonal modules (i.e., shoots and buds) per stem produced from (**A**) the new basal meristematic zone, counted as the first "node," which consisted of a nodular agglomeration formed consistently at ~2 cm from the new surface, regardless of treatment; (**B**) second and third nodes below the base; and (**C**) fourth and lower nodes in *S. anglica* plants subjected to surface displacement of 8 and 16 cm above the original marsh surface. Results are presented as box plots (*9*), each consisting of a box, divided at the median, whose left- and right-hand sides are drawn at the lower and upper quartiles. Dotted lines are drawn from the lower and upper quartiles to the smallest and largest observations within 1.5 interquartile ranges of each side of the box. All further values are plotted individually (×). Abundant roots of different diameters, ranging down to small filaments, also emerged from the new base. Modules forming from subsequent individual nodes below the base (nodes 2, 3, 4, etc.) were separated by internodal stem sections >1 cm long.

References and Notes

1. A. C. Redfield, *Science* **147**, 50 (1965).
2. A. J. Gray, D. F. Marshall, A. F. Raybould, *Adv. Ecol. Res* **21**, 1 (1991).
3. P. J. Goodman, W. T. Williams, *J. Ecol.* **49**, 391 (1961).
4. Further information on methods and data are available as supporting material on *Science* Online.
5. I. A. Mendelssohn, N. L. Kuhn, *Ecol. Eng.* **21**, 115 (2003).
6. K. L. McKee, W. H. Patrick Jr., *Estuaries* **11**, 143 (1988).
7. J. T. Morris, C. Haley, R. Krest, in *Biological and Environmental Chemistry of DMSP and Related Sulfonium Compounds*, R. Kiene, P. Vissher, M. Keller, G. Kirst, Eds. (Plenum, New York, 1996), pp. 87–95.
8. J. T. Morris, J. W. H. Dacey, *Am. J. Bot.* **71**, 979 (1984).
9. J. W. Tukey, *Exploratory Data Analysis* (Addison-Wesley, Reading, MA, 1977).
10. We thank H. Gillett, A. Hayes, F. Hughes, J. Scharlemann, M. Tester, and H. Viles for helpful discussions and support.

Supporting Online Material

www.sciencemag.org/cgi/content/full/322/5904/1064/DC1
Materials and Methods
Tables S1 and S2

2 May 2008; accepted 9 September 2008
10.1126/science.1159973

[1]United Nations Environmental Programme–World Conservation Monitoring Centre (UNEP-WCMC), 219 Huntingdon Road, Cambridge CB3 0DL, UK. [2]Cambridge Coastal Research Unit, Department of Geography, University of Cambridge, Cambridge CB2 3EN, UK.

*To whom correspondence should be addressed. E-mail: gerardo.fragoso@unep-wcmc.org

Reconstruction of Zebrafish Early Embryonic Development by Scanned Light Sheet Microscopy

Philipp J. Keller,[1,2]* Annette D. Schmidt,[2] Joachim Wittbrodt,[1,2,3,4]* Ernst H.K. Stelzer[1]

A long-standing goal of biology is to map the behavior of all cells during vertebrate embryogenesis. We developed digital scanned laser light sheet fluorescence microscopy and recorded nuclei localization and movement in entire wild-type and mutant zebrafish embryos over the first 24 hours of development. Multiview in vivo imaging at 1.5 billion voxels per minute provides "digital embryos," that is, comprehensive databases of cell positions, divisions, and migratory tracks. Our analysis of global cell division patterns reveals a maternally defined initial morphodynamic symmetry break, which identifies the embryonic body axis. We further derive a model of germ layer formation and show that the mesendoderm forms from one-third of the embryo's cells in a single event. Our digital embryos, with 55 million nucleus entries, are provided as a resource.

Model systems such as *Caenorhabditis elegans* and *Ciona intestinalis* lend themselves well to comprehensive analyses at the cellular level, for example, by conventional microscopy (*1*, *2*). However, global studies of complex vertebrate species encounter technical limitations. Whereas the formation of single organs has been reconstructed by imaging and tracking nuclear fluorescent proteins for several hours (*3*–*6*), obtaining quantitative morphogenetic data representing the full embryos over the entire time course of embryogenesis remains a major challenge.

For comparison, 671 cells need to be followed during *C. elegans* embryogenesis, whereas the analysis of complex vertebrate embryos requires the simultaneous tracking of tens of thousands of cells. High spatiotemporal resolution, ultralow photobleaching rates, and an excellent signal-to-noise ratio are crucial. In order to follow the nuclei of the 16,000 cells of an 18-hour-old zebrafish embryo, a volume of 1000 by 1000 by 1000 μm^3 must be recorded at least once every 90 s because nuclei move several micrometers per minute. In order to reliably detect all nuclei, the set of images must be acquired at a step size of no more than 3 μm along the z axis, resulting in ~350 images per time point. In addition, an image size of at least 1500 by 1500 pixels is necessary to elucidate nuclear morphologies. Thus, the observation must be performed at a continuous imaging speed of at least 10 million volume elements (voxels) per second. A dynamic range of at least 12 bit covers the varying expression levels of genetically encoded markers. At the same time, photobleaching and phototoxicity (*7*) must be minimized to ensure the physiological development of the embryo. Finally, the embryo's central yolk cell is opaque at physiological wavelengths; therefore, imaging along multiple directions is needed to capture the development of the entire embryo.

The most widely applied advanced fluorescence imaging techniques rely on confocal and multiphoton microscopes, which provide three-dimensional resolution but lack the combination of high-speed imaging and low phototoxicity required for the fast recording of entire embryos over long periods of time. They are also unsuited for multiview imaging (*8*). To overcome some of these limitations, we recently introduced light sheet–based technologies to biological imaging (SPIM) (*9*). With these microscopes, the specimen is illuminated along a single plane with a sheet of light that is typically generated via a set of apertures and by focusing a collimated beam with a cylindrical lens. This arrangement provides three-dimensional optical sectioning and reduces the energy load on the specimen (*9*–*11*).

Digital scanned laser light sheet fluorescence microscopy. To achieve the imaging speed and quality for recording entire embryos, we developed digital scanned laser light sheet fluorescence microscopy (DSLM) (fig. S1). The idea behind DSLM is to generate a "plane of light" with a laser scanner that rapidly moves a micrometer-thin beam of laser light vertically and horizontally through the specimen (Fig. 1 and movie S1).

This approach has several advantages over standard light sheet microscopy. First, DSLM illuminates each line in the specimen with the same intensity, a crucial prerequisite for quantitative imaging of large specimens (fig. S2). Second, in contrast to standard light sheet–based microscopy, DSLM does not rely on apertures to form the laser profile, which reduces optical aberrations and thereby provides an exceptional image quality. Third, the entire illumination power of the light source is focused into a single line, resulting in an illumination efficiency of 95% as compared with ~3% in standard light sheet microscopy. Fourth, DSLM allows to generate intensity-modulated illumination patterns (structured illumination) (*12*), which can be used to enhance the image contrast in highly light-scattering specimens, such as large embryos. Furthermore, DSLM combines (i) an imaging speed of 63 million voxels per second, (ii) a signal-to-noise ratio of 1000:1 at a lateral and axial resolution of 300 and 1000 nm, respectively, and (iii) ultralow excitation energies confined to a single plane (1.7 μJ at 488 nm passing each plane in our zebrafish experiments) (*8*).

In order to analyze zebrafish embryonic development, we recorded stacks of ~400 images (2048 by 2048 pixels each) in intervals of 60 or 90 s and along two opposing directions (Fig. 2 and movies S2 and S3). The embryos were embedded in agarose, kept at a constant temperature (26.5°C) [see (*13*) for developmental stages] throughout the experiment, and exhibited normal development (*8*). Nuclei were labeled at the one-cell stage by mRNA injection of H2B-eGFP, a fusion protein of human histone-2B and the en-

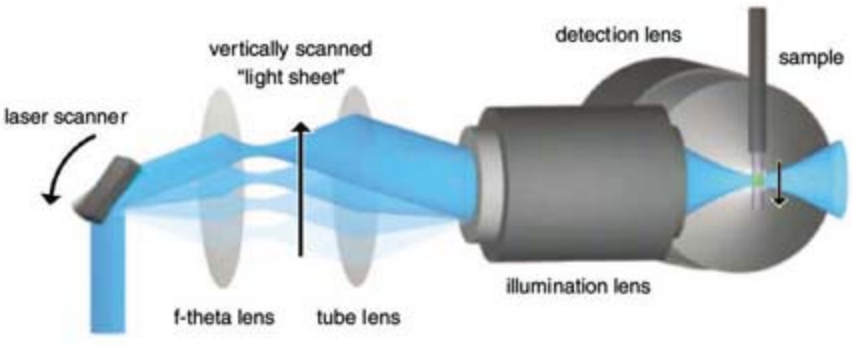

Fig. 1. Digital scanned laser light sheet microscopy. The laser beam illuminates the specimen from the side and excites fluorophores along a single line. Rapid scanning of a thin volume and fluorescence detection at a right angle to the illumination axis provides an optically sectioned image (movie S1). The f-theta lens converts the tilting movement of the scan mirror into a vertical displacement of the laser beam. The tube lens and the illumination objective focus the laser beam into the specimen, which is positioned in front of the detection lens.

[1]Cell Biology and Biophysics Unit, European Molecular Biology Laboratory (EMBL), Meyerhofstrasse 1, D-69117 Heidelberg, Germany. [2]Developmental Biology Unit, EMBL, Meyerhofstrasse 1, D-69117 Heidelberg, Germany. [3]Institute of Zoology, Department for Developmental Physiology, University of Heidelberg, INF 230, D-69120 Heidelberg, Germany. [4]Institute of Toxicology and Genetics, Karlsruhe Institute of Technology (KIT), Post Office Box 3640, D-76021 Karlsruhe, Germany.

*To whom correspondence should be addressed. E-mail: keller@embl.de (P.J.K.), wittbrod@embl.de (J.W.)

hanced green fluorescent protein (GFP) reporter, which localizes to chromatin (*14*). This presents an effective marker for cell positions and cell divisions because changes in chromatin density can be directly observed. Imaging was performed for 24 hours, providing about 400,000 images per embryo.

We measured nuclear fluorescence intensities and found that steady-state GFP concentrations are reached at ~12 hours post fertilization (hpf), owing to the limited stability of the injected mRNA. However, despite continuous imaging for another 12 hours, the fluorescence intensity levels remained constant. This indicates a negligible photobleaching rate in DSLM high-speed live imaging (fig. S3). We applied comparable experimental settings in state-of-the-art confocal and two-photon fluorescence microscopes. The embryo was exposed to a factor of 5600 more energy in the confocal (9.6 mJ at 488 nm passing each plane) and to a factor of 10^6 more energy in the two-photon fluorescence microscope (1.7 J at 930 nm passing each plane) (*8*). Thus, DSLM allows for a comprehensive, quantitative analysis of zebrafish embryonic development, over periods longer than 24 hours, with high spatiotemporal resolution and ultralow phototoxicity.

The digital embryo. To efficiently handle the large amounts of microscopy data, we developed a parallelized image segmentation pipeline, i.e., a set of software modules that automatically detects nuclei in the raw images by using large-scale computer networks (at the European Molecular Biology Laboratory, EMBL; and Karlsruhe Institute of Technology, KIT) (fig. S4). Image segmentation was performed by (i) recursive refinement of the three-dimensional shapes and internal structures of objects detected in the microscopy data (fig. S5), (ii) subsequent filtering of these objects according to the morphological characteristics expected for nuclei, and (iii) an analysis of the identification rate for each nucleus throughout time (*8*). Because of the high signal-to-noise ratio of the DSLM data, we obtained a robust average segmentation efficiency of 97% during the first 10 hours of embryogenesis and an average of 90% during late gastrulation (*8*). The microscopy data acquired along the two opposing directions were segmented separately and subsequently combined into a complete data set by a fusion algorithm (*8*). A "digital embryo" was derived for each experiment and constitutes a comprehensive database of the positions, sizes, and fluorescence intensities of 92% of the nuclei in the entire embryo (determined by manual controls) (*8*) throughout early embryogenesis from early cleavage stages up to the onset of heartbeat (Fig. 2 and movie S3). The algorithms, furthermore, provide 99.5% efficiency in converting these nuclear positions into migratory tracks, corresponding to one tracking error per 200 time points or 3 to 5 hours (*8*). We processed seven 24-hour time-lapse recordings of zebrafish embryogenesis and obtained developmental blueprints with 55 million nuclear data entries, including a reconstruction of the zebrafish *one-eyed pinhead* mutant (*MZoep*) (*15*). Our data on zebrafish embryogenesis from 1.5 to 30 hpf are presented as time-lapse movies of the microscopy recordings (movies S2, S4, S7, and S12) and as movies of the reconstructions (movies S3, S5, S8, and S13). Further analysis of the digital embryos (*8*) provides a detailed description of morphogenetic and developmental processes at subcellular resolution (fig. S3), spatiotemporal coordinates and polarity of cell divisions (movie S10 and Fig. 3B and fig. S6), global nuclear population statistics (figs. S3 and S6), embryo-to-embryo variability in morphogenetic key parameters (fig. S7), and cell tracking throughout development (movies S9, S11, S14, and S15 and Fig. 3A).

The digital embryos provide direct quantitative access to a global analysis of cell and tissue behavior, as shown below. In order to visualize morphogenetic domains, we tracked individual cell movements up to somitogenesis stages and color-encoded the information on directionality (movies S9, S14, and S15 and Fig. 3A). This analysis identifies morphogenetic movements during development (emboly, epiboly, convergence, and extension) and provides a global, quantitative perspective of their interplay.

Early morphodynamic symmetry-breaking. Nuclear β-catenin is one of the earliest markers for the future dorsal side of the embryo (~512-cell stage) (*16*, *17*), which raises the question of whether morphodynamic symmetry-breaking also occurs at this early time point. We mapped and analyzed the three-dimensional patterns and polarity of early cell divisions in five embryos during 1.5 to 7 hpf [all experiments were per-

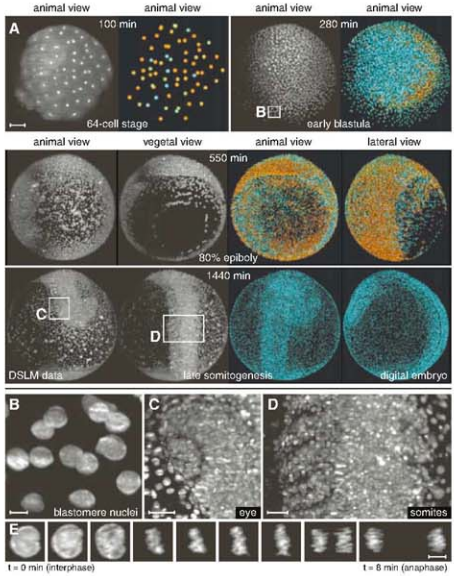

Fig. 2. Imaging and reconstruction of zebrafish embryogenesis. **(A)** Maximum-intensity projections (left) and digital embryo reconstructions (right) of nuclear-labeled wild-type zebrafish embryo (movies S2 and S3) at the indicated times and developmental stages. Color code: movement speeds (0 to 1.2 μm/min, cyan to orange). Images are Lucy-Richardson-deconvolved (10 iterations). Zeiss C–Apochromat 10x/0.45. Scale bar, 100 μm. (**B** to **D** insets and parts) Frames of close-ups on (A), demonstrating subcellular resolution of various areas of the developing embryo. Enlargements scale bar, 10 μm (B), 30 μm (C and D). **(E)** Nuclear morphology of a dividing blastomere from movie S7 (intensity-normalized). Scale bar, 10 μm. *t*, time.

formed at 26.5°C (*13*)] (movie S10). Whereas planes of cell division are evenly distributed [fig. S6b; in contrast to the asymmetry in gastrulation (*18*, *19*)], a symmetry break in the spatiotemporal pattern occurs at the 512-cell stage (movie S10 and Fig. 4A). Initially, cell divisions follow 3-min-long radial waves, originating in the embryonic center. After the 512-cell stage, two circular peripheral waves break this radial symmetry (Fig. 4, A and B, and fig. S8 and movie S10). They occur during division cycles 10 to 13 at an angle that correlates with the future body axis (Fig. 4B).

To investigate whether the break of radial symmetry can also be related to nuclear densities, we determined the nuclear counts in small volumes around the animal pole. This analysis indicates a divergence commencing at 5 hpf, i.e., two hours after the symmetry break in cell division patterns, but still before the morphological signs of shield formation at the onset of convergence (8 hpf) (Fig. 4C). Between 5 and 8 hpf, reduced cell proliferation rates in the future embryonic shield result in lower cell densities dorsally (rather than dorsal compaction) (*20*, *21*) and, thereby, indicate the position of the future body axis.

Thus, by dissecting the three-dimensional pattern of cell divisions in the entire embryo, we reveal an early morphodynamic symmetry break, concomitant with the nuclear localization of β-catenin, that allows an early prediction of the orientation of the body axis, preceding the midblastula transition (*22*).

A model of hypoblast formation. In addition to enabling the analysis of global quantitative studies, the digital embryos allow us to focus on confined morphogenetic events. We investigated the formation of the hypoblast, the inner cell layer, which gives rise to mesoderm and endoderm. The formation of the hypoblast is known to result from internalization of cells (emboly) of the outer layer (epiblast) during gastrulation and stretching and thinning of cell sheets over the yolk (epiboly) (*23*). Our data

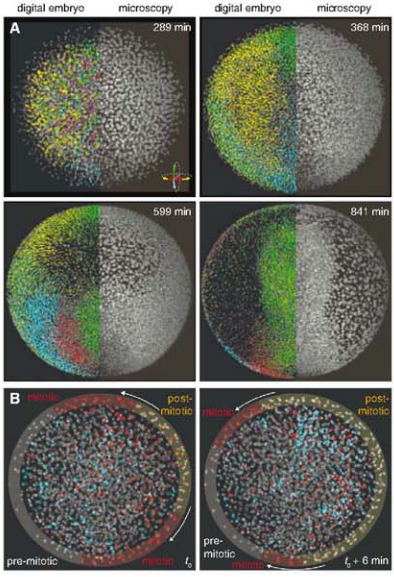

Fig. 3. Cell tracking and detection of cell divisions in the digital embryo. **(A)** Microscopy data (right half of embryo: animal view, maximum projection) and digital embryo (left half of embryo) with color-encoded migration directions (see movie S9). Color code: dorsal migration (cyan), ventral migration (green), toward or away from body axis (red or yellow), toward yolk (pink). **(B)** Dividing cells (red) and their daughter cells (blue). See movie S10 and fig. S6b for complete coverage (1.7 to 6.7 hpf). Yellow, red, and gray overlays indicate progression of the peripheral cell division waves during division cycle 12 (arrows show direction of peripheral waves; t_0 = 216 min, see also Fig. 4).

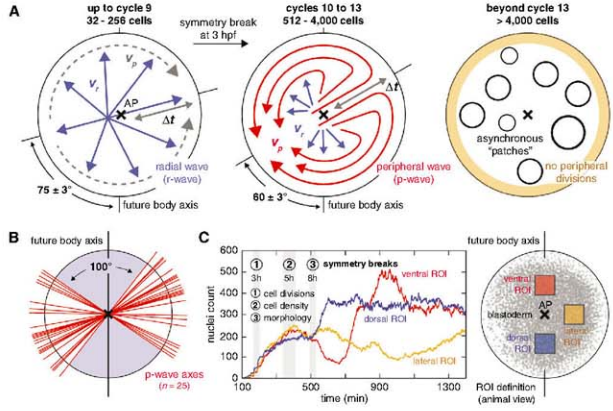

Fig. 4. Symmetry-breaking of the global cell division pattern. **(A)** Illustration of the cell division patterns during early zebrafish embryogenesis: fast radial waves (cycles 1 to 9, progression speed v_r), slow circular peripheral waves (cycles 10 to 13, progression speed v_p), and asynchronous cell-division patches (cycles 14+). Errors are indicated as SEM. A quantification of the parameters v_r, v_p, and the time shift Δt between radial and peripheral waves is provided in fig. S8. **(B)** Symmetry axes of 25 peripheral waves (20 slow waves in cycles 10 to 13 and 5 fast waves in cycle 9; n = 5 embryos). Of the 25 waves, 92% occurred at an angle of 45 to 90° to the future body axis. **(C)** Nuclei counts in three 110 by 110 μm^2 domains (future dorsal, ventral, and lateral) reveal the first symmetry break in cell densities at 5 hpf. The symmetry break in the cell division pattern (3 hpf) precedes the symmetry break in cell densities (5 hpf) and the first morphogenetic symmetry break (onset of convergence, 8 hpf).

reveal a pronounced "embolic wave" of internalization and regional differences in modes of internalization (Fig. 5 and fig. S9 and movies S14 and S15).

Starting at 5.8 hpf (40% epiboly at 26.5°C) (*13*) and lasting for 2 hours, ~1550 cells (34% of all cells) internalize around the perimeter of the blastopore to form the mesendoderm (Fig. 5 and fig. S9). After this time window, we did not observe any further cells moving from epiblast to hypoblast.

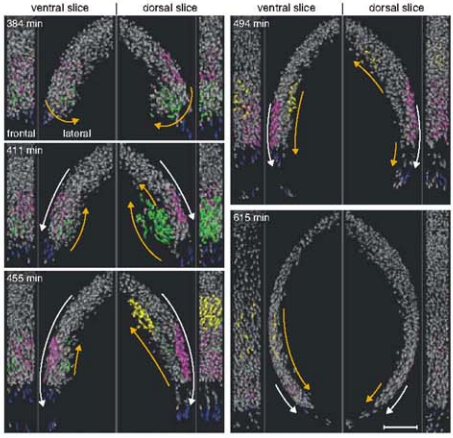

Fig. 5. Mesendoderm internalization and migration in dorsal and ventral hemispheres. Frontal and lateral views of slices on dorsal (shield region, right) and ventral hemispheres (opposite of shield, left). Four cell populations were tracked (movie S16): green or yellow nuclei in the early or late embolic wave, blue nuclei at the leading edge of epiboly, and noninternalizing pink nuclei. Orange and white arrows indicate hypoblast and epiblast cell movements. Scale bar, 100 μm.

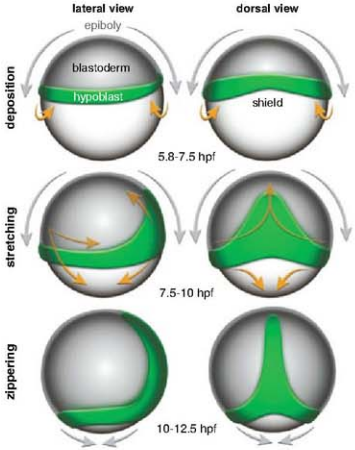

Fig. 6. A model of mesendoderm formation in zebrafish. The hypoblast forms in a single synchronized internalization wave around the entire circumference ("deposition"). On the dorsal side, internalized cells become distributed along the entire future body axis ("stretching"). On the ventral side, the internalized ring of hypoblast cells moves toward the vegetal pole. The ring closes at the vegetal pole ("zippering") and completes the formation of the hypoblast. Orange arrows indicate hypoblast cell movements. Gray arrows indicate epiboly.

Internalizing cells follow the path of a wave, which stretches inward toward the yolk cell, reaches a peak height of 50 μm before rolling over, touches the deep cells situated closer to the animal pole (Fig. 5, green cell population, and movie S16), and completes emboly at 7.5 hpf. Whereas cells internalize around the entire perimeter, the wave is most prominent dorsally. The onset of internalization is synchronized along the blastopore (fig. S9, c and d), but the folding-over at the dorsal shield takes 30 min longer than at other locations along the blastopore. As a consequence of this dorsally pronounced emboly, the dorsal leading edge of epiboly lags behind in its vegetal approach (movie S14).

Modes of internalization (*24*), either involution (synchronously flowing sheets as in amphibian gastrulation) or ingression (cells individually sinking inward), have been subject to intense discussion (*25*, *26*). To determine whether modes of internalization vary regionally, we generated "internalization maps" for the dorsal and ventral hemispheres (fig. S9a). An analysis of time shifts between internalization events around the blastopore reveals that asynchronous internalization and radial intercalation of single cells in the shield region disrupt the internalization pattern on the dorsal hemisphere [fig. S9, b and e; supporting previous single cell–tracking studies (*27*, *28*)]. On the ventral hemisphere, however, mesendoderm internalization occurs exclusively in a synchronous manner (fig. S9, b and e), reminiscent of involution (*24*) or an intermediate mechanism termed "synchronized ingression" (*23*, *29*).

In dorso-anterior regions on the animal hemisphere, internalized cells move antiparallel to epiblast cells toward the animal pole for ~100 min (Fig. 5, purple and yellow cell populations; movie S14). In contrast, internalized cells in the ventral hemisphere change direction within 30 min after internalization and migrate toward the vegetal pole (Fig. 5 and movies S15 and S16).

Unlike gastrulation in *Xenopus* (*30*), a continuous rolling internalization with hypoblast cells moving toward the animal pole does not occur as epiboly proceeds to the vegetal hemisphere (movie S16). Instead, hypoblast cells follow a well-defined leading edge and move parallel to epiblast cells toward the vegetal pole (movie S14, *xz* slice).

A comparative reconstruction of the zebrafish M*Zoep* mutant quantitatively describes its deficiency in forming mesendoderm (*15*, *27*): Whereas ~1550 cells internalize via the embolic wave in the wild-type embryo, the M*Zoep* digital embryo (movies S4 and S5) reveals merely ~60 internalizing cells in the entire embryo during the same time period (movie S6). This visualization shows that the oversized epiblast (*15*) forms through convergence and absence

of internalization and dorsal stretching (movies S5 and S6). Convergence is highly abnormal and prolonged, with ventral cells moving across the animal pole toward the epiblast's center (movie S6).

In conclusion, we show that wild-type hypoblast cells are deposited in a single embolic wave that occurs before epiboly moves the blastopore to the vegetal hemisphere. The embryo is therefore split into a dorso-anterior domain characterized by antiparallel movements of germ layers and a dorso-posterior domain, where the parallel migration of epi- and hypoblast stretches the hypoblast. In the trunk and tail regions, parallel germ layer migration and convergence and/or extension move the mesendoderm, deposited in a ring around the blastopore, to an axial position, closing the blastopore dorsally from anterior to posterior like a zipper.

Our analysis puts previous cell-tracking studies (*31*, *32*) into a global perspective. Regarding mesendoderm formation in zebrafish, a three-stage model is proposed (Fig. 6): Mesendoderm forms by (i) global deposition in a single event, (ii) dorsal stretching, and (iii) anteroposterior "zippering."

Different modes of internalization characterize the initial deposition, with synchronous events (involution and/or synchronized ingression) occurring on the ventral side, and disruption of synchrony (asynchronous ingression and/or radial intercalation) on the dorsal side. Our analysis of the entire embryo describes the migratory behavior of 92% of all cells throughout gastrulation and leads to a comprehensive model that complements and partially revises the general view of zebrafish gastrulation (*30*, *33*). In particular, our finding of a single embolic event contradicts the current assumption of a continuous internalization during epiboly (*30*, *33*–*35*).

Conclusions. We developed and applied DSLM as a fluorescence microscopy system for the high-speed in vivo observation of embryonic development at subcellular resolution, which enabled cell tracking in the entire early zebrafish embryo. Applying the automated image segmentation pipeline provides a "digital embryo" that visualizes complex developmental events in a global context. We demonstrate application of the method to a quantitative reconstruction of early cell division patterns. This analysis reveals an initial morphodynamic symmetry break, before the onset of zygotic transcription, coinciding with the embryonic body axis. We also follow germ layer formation on a quantitative level and provide a comprehensive model of hypoblast formation in zebrafish embryos. We show that the mesendoderm forms from one-third of the embryo's cells in a single embolic event by means of regionally different modes of internalization.

Our digital embryos constitute complex data sets with information about millions of nuclear positions, as well as thousands of cell tracks and cell divisions per embryo. These data are publicly available in a central repository as a resource for further analyses (*36*).

Detailed recordings of embryonic development will allow the measurement and the modeling of the mechanical forces that drive morphogenesis, e.g., by complementing existing data with information about membrane dynamics. Further applications range from the construction of databases of organ development (using tissue-specific fluorescent lines) and the analysis of mutant phenotypes (*37*–*39*) to the quantification of the variability of vertebrate cell lineages. Moreover, with its high-throughput and high-content capabilities DSLM presents a powerful tool for systems biology and enables complete in vivo reconstructions of gene expression dynamics that incorporate the steadily growing number of gene and enhancer trap lines (*40*–*42*). In addition, DSLM should be suitable for analyses of entire mouse, chicken, and *Xenopus* early embryogenesis—the unfavorable light-scattering tissue properties of *Xenopus* can be partially overcome by DSLM's intrinsic structured illumination and multiview imaging capabilities. The comparison of individuals within species and across species borders might allow us to reveal the conserved and emerging morphogenetic rules of embryogenesis.

References and Notes

1. J. E. Sulston, E. Schierenberg, J. G. White, J. N. Thomson, *Dev. Biol.* **100**, 64 (1983).
2. P. Lemaire, *Science* **312**, 1145 (2006).
3. Y. Hirose, Z. M. Varga, H. Kondoh, M. Furutani-Seiki, *Development* **131**, 2553 (2004).
4. M. Rembold, F. Loosli, R. J. Adams, J. Wittbrodt, *Science* **313**, 1130 (2006).
5. S. J. England, G. B. Blanchard, L. Mahadevan, R. J. Adams, *Development* **133**, 4613 (2006).
6. S. G. Megason, S. E. Fraser, *Cell* **130**, 784 (2007).
7. R. Y. Tsien, L. Ernst, A. Waggoner, in *Handbook of Biological Confocal Microscopy*, J. B. Pawley, Ed. (Springer, New York, 2006), pp. 338–352.
8. Materials and methods are available as supporting material on *Science* Online.
9. J. Huisken, J. Swoger, F. Del Bene, J. Wittbrodt, E. H. Stelzer, *Science* **305**, 1007 (2004).
10. P. J. Keller, F. Pampaloni, E. H. Stelzer, *Curr. Opin. Cell Biol.* **18**, 117 (2006).
11. P. J. Keller, F. Pampaloni, E. H. Stelzer, *Nat. Methods* **4**, 843 (2007).
12. M. A. Neil, R. Juskaitis, T. Wilson, *Opt. Lett.* **22**, 1905 (1997).
13. K. K. Hisaoka, H. I. Battle, *J. Morphol.* **102**, 311 (1958).
14. T. Kanda, K. F. Sullivan, G. M. Wahl, *Curr. Biol.* **8**, 377 (1998).
15. K. Gritsman *et al.*, *Cell* **97**, 121 (1999).
16. S. Schneider, H. Steinbeisser, R. M. Warga, P. Hausen, *Mech. Dev.* **57**, 191 (1996).
17. S. T. Dougan, R. M. Warga, D. A. Kane, A. F. Schier, W. S. Talbot, *Development* **130**, 1837 (2003).
18. M. L. Concha, R. J. Adams, *Development* **125**, 983 (1998).
19. Y. Gong, C. Mo, S. E. Fraser, *Nature* **430**, 689 (2004).
20. R. M. Warga, C. Nusslein-Volhard, *Dev. Biol.* **203**, 116 (1998).
21. B. Schmitz, I. A. Campos-Ortega, *Rouxs Arch. Dev. Biol.* **203**, 374 (1994).
22. D. A. Kane, C. B. Kimmel, *Development* **119**, 447 (1993).
23. L. Solnica-Krezel, *Curr. Biol.* **15**, R213 (2005).
24. J. P. Trinkaus, *Cells into Organs: The Forces That Shape the Embryo* (Prentice-Hall, Englewood Cliffs, NJ, ed. 2, 1984).
25. D. Kane, R. J. Adams, in *Pattern Formation in Zebrafish*, L. Solnica-Krezel, Ed. (Springer, Heidelberg, 2002).
26. L. A. Rohde, C. P. Heisenberg, *Int. Rev. Cytol.* **261**, 159 (2007).
27. J. A. Montero *et al.*, *Development* **132**, 1187 (2005).
28. J. Shih, S. E. Fraser, *Development* **121**, 2755 (1995).
29. R. J. Adams, C. B. Kimmel, in *Gastrulation: From Cells to Embryo*, C. D. Stern, Ed. (Cold Spring Harbor Laboratory Press, Cold Spring Harbor, NY, 2004), pp. 305–316.
30. L. Wolpert, *Principles of Development* (Oxford Univ. Press, New York, ed. 3, 2007).
31. D. C. Myers, D. S. Sepich, L. Solnica-Krezel, *Dev. Biol.* **243**, 81 (2002).
32. D. S. Sepich, C. Calmelet, M. Kiskowski, L. Solnica-Krezel, *Dev. Dyn.* **234**, 279 (2005).
33. S. F. Gilbert, *Developmental Biology* (Sinauer Associates, Sunderland, MA, ed. 8, 2006).
34. R. M. Warga, C. B. Kimmel, *Development* **108**, 569 (1990).
35. G. Pezeron *et al.*, *Curr. Biol.* **18**, 276 (2008).
36. Movies and zebrafish digital embryos can be downloaded at www.embl-heidelberg.de/digitalembryo
37. D. A. Kane *et al.*, *Development* **123**, 47 (1996).
38. C. P. Heisenberg, M. Tada, *Semin. Cell Dev. Biol.* **13**, 471 (2002).
39. D. S. Sepich, L. Solnica-Krezel, *Methods Mol. Biol.* **294**, 211 (2005).
40. S. Ellingsen *et al.*, *Development* **132**, 3799 (2005).
41. S. Parinov, I. Kondrichin, V. Korzh, A. Emelyanov, *Dev. Dyn.* **231**, 449 (2004).
42. K. Asakawa *et al.*, *Proc. Natl. Acad. Sci. U.S.A.* **105**, 1255 (2008).

43. We thank U. Liebel, M. Alef, and M. Wahlers for excellent KIT/EMBL computer cluster support; the EMBL mechanical workshop for custom hardware; A. Riedinger and G. Ritter for custom electronics; F. Härle and A. Riedinger for custom microscope operating software; W. Dilling for technical drawings; M. Knop, K. Brown, K. Khairy, J. Martinez, D. Gilmour, and C.-P. Heisenberg for critical manuscript comments; L. Centanin for immunostained medaka embryos; C.-P. Heisenberg for MZ*oep* mutants; S. Terjung for Leica SP5 support; G. Giese for Zeiss LSM 510 NLO support. Financial support: EU-FP6-STREP Plurigenes, DFG SFB-488 (J.W.); Studienstiftung des deutschen Volkes (P.J.K.); Hartmut Hoffmann-Berling International Graduate School of Molecular and Cellular Biology, HBIGS (A.D.S.). Contributions: P.J.K. outlined the digital embryo project, designed and built the DSLM, recorded the microscopy data, developed the image processing pipeline, performed the reconstructions and drafted the manuscript. A.D.S. developed the biological methods, performed the biological preparations, contributed to project planning and participated in the writing of the manuscript. E.H.K.S. outlined the DSLM development, cosupervised the project, and participated in manuscript preparation. P.J.K., A.D.S., and J.W. analyzed the digital embryos. J.W. guided the biological research, cosupervised the project, and participated in the writing of the manuscript.

Supporting Online Material

www.sciencemag.org/cgi/content/full/1162493/DC1
Materials and Methods
Figs. S1 to S9
References
Movies S1 to S16

30 June 2008; accepted 1 October 2008
Published online 9 October 2008;
10.1126/science.1162493
Include this information when citing this paper.

Kinetics of Individual Nucleation Events Observed in Nanoscale Vapor-Liquid-Solid Growth

B. J. Kim,[1] J. Tersoff,[2] S. Kodambaka,[2]* M. C. Reuter,[2] E. A. Stach,[1]† F. M. Ross[2]†

We measured the nucleation and growth kinetics of solid silicon (Si) from liquid gold-silicon (AuSi) catalyst particles as the Si supersaturation increased, which is the first step of the vapor-liquid-solid growth of nanowires. Quantitative measurements agree well with a kinetic model, providing a unified picture of the growth process. Nucleation is heterogeneous, occurring consistently at the edge of the AuSi droplet, yet it is intrinsic and highly reproducible. We studied the critical supersaturation required for nucleation and found no observable size effects, even for systems down to 12 nanometers in diameter. For applications in nanoscale technology, the reproducibility is essential, heterogeneity promises greater control of nucleation, and the absence of strong size effects simplifies process design.

Nucleation is central to all types of growth phenomena, but it is a fleeting event and thus difficult to observe in detail. Phase transitions in macroscopic samples typically involve a large number of distinct nucleation events, and the properties of the final material (such as grain-size distribution) are determined by the statistical ensemble of nucleation events. However, systems that are sufficiently small will transform by a single nucleation event. This raises issues such as statistical variability and size effects (*1*–*3*). These classic issues take on new urgency in the context of nanoscale technology, in which an entire functional structure such as a nanowire transistor may depend on a single nucleation event. Only recently, using innovative microscopy techniques, has it become feasible to study individual nucleation events in nanoscale systems (*4*–*10*).

We used ultrahigh-vacuum transmission electron microscopy (UHV-TEM) to examine the growth of Si from a AuSi eutectic liquid, a system of particular relevance for the initial stages of nanowire growth by the vapor-liquid-solid process (VLS) (*11*) and one in which devices such as wrap-gate field-effect transistors have been demonstrated (*12*–*14*). By comparing quantitative measurements of nucleation and growth with a simple kinetic model, we determined the critical supersaturation of Si in AuSi required for nucleation and explained in detail the subsequent growth kinetics. Hofmann *et al.* (*10*) recently reported in situ observations of nucleation and growth in a similar system, addressing the "incubation time" for nucleation, which primarily reflects the vapor-liquid kinetics and is not sensitive to the nucleation process. Here, we have extracted key information about the nucleation process itself, which allows us to examine size effects and reproducibility, both of which are important for a fundamental understanding of nucleation and for reliable fabrication of nanowires for applications.

[1]School of Materials Engineering and Birck Nanotechnology Center, Purdue University, West Lafayette, IN 47907, USA. [2]IBM Research Division T. J. Watson Research Center, Yorktown Heights, NY 10598, USA.

*Present address: Department of Materials Science and Engineering, University of California Los Angeles, Los Angeles, CA 90095, USA.

†To whom correspondence should be addressed. E-mail: eastach@purdue.edu (E.A.S.); fmross@us.ibm.com (F.M.R.)

Experiments were carried out in a UHV-TEM that is equipped with facilities for introducing the reactive gas disilane (Si_2H_6) to a heated sample while it remains under observation (*15*–*17*). Nucleation and growth kinetics of Si were observed in nanoscale Au crystallites supported on an electron-transparent amorphous SiN_x membrane. Figure 1 shows a series of images as a function of disilane exposure time, showing the initial transformation of polycrystalline Au islands (Fig. 1A) into eutectic droplets of AuSi (Fig. 1B), followed by the appearance of Si nuclei (Fig. 1C). Enlargements in Fig. 1, D to F, show one reaction sequence in more detail, and movies S1 and S2 illustrate a complete video sequence and a magnified view of a single nucleation event. The general behavior is consistent with that reported in (*10*), but we took advantage of time-resolved measurements to focus on the kinetics of the initial nucleation. In all cases, we found that Si nucleation occurs at the edge of the droplet, which suggests that this is the energetically favorable location that minimizes the nucleation barrier (*18*). At later times, the Si nuclei grew into elongated wires. We did not analyze this stage of growth because of the random wire direction and geometry, but instead focused on the regime in which the nuclei are still small particles within the AuSi droplets.

Figure 2A shows a representative series of images of a Si nucleus after formation, and Fig. 2,

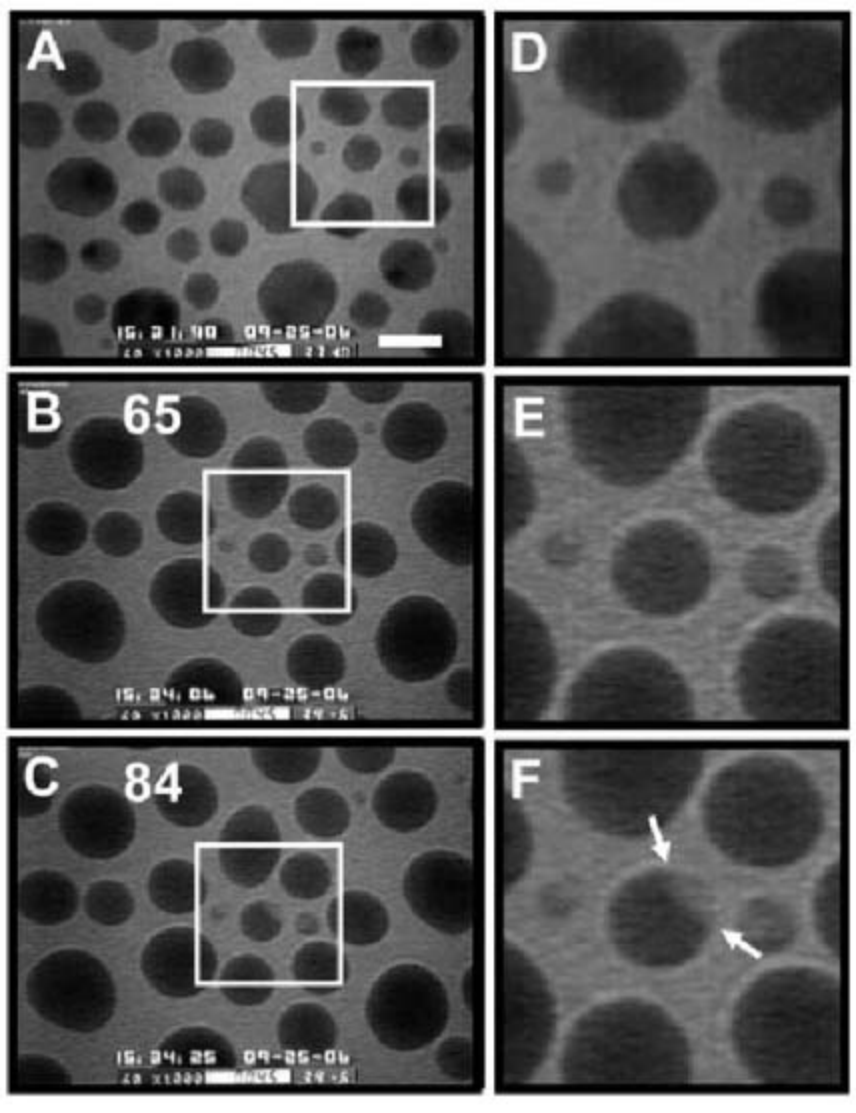

Fig. 1. (**A** to **C**) Bright-field images extracted from a video obtained during nucleation of Si from polycrystalline Au clusters at 525°C and 4×10^{-6} torr disilane. Scale bar, 20 nm. (A) Image acquired before opening the leak valve, showing polycrystalline Au particles, as indicated by their faceted shapes and by the interparticle variations in their bright-field contrast. (B) Image acquired after 65 s, showing the formation of the liquid AuSi alloy as reflected by the rounded shapes in projection and the disappearance of crystalline contrast. (C) Image acquired after 84 s, showing the appearance of a Si nucleus with lighter contrast at the edge of one AuSi droplet. (**D** to **F**) Enlarged images of the boxed regions of (A) to (C), respectively. Arrows in (F) indicate the interface between liquid AuSi and solid Si.

B and C, shows quantitative measurements of the radius r (defined in the figure caption) versus time t of this and several other nuclei obtained at 525°C from droplets of different volumes at two different pressures. The data show that after disilane was introduced at $t = 0$, a certain time elapsed (the incubation time) before the solid Si nucleus appeared. Each nucleus initially grew very rapidly but within a few seconds reached a crossover point (C), after which the growth slowed down. This crossover is visibly sharper at lower pressures, as seen by comparing Fig. 2, B and C. Larger droplets show a longer incubation time, as expected from scaling arguments (*10*, *19*), and also show a larger initial jump in nucleus size.

To model these kinetics, we used the fact that disilane cracking on the droplet surface results in a steady supply of Si into the droplet, which causes the Si fraction within the droplet to increase continuously. This initially results in a transition from solid pure Au to a liquid AuSi alloy. As more Si is supplied, the mole fraction of Si in the AuSi liquid alloy increases. At thermodynamic equilibrium, solid Si would appear when the AuSi composition (c) reaches the Si liquidus composition at the growth temperature (c_0). However, for growth on a substrate different from Si, there is a nucleation barrier to form the new crystalline Si phase. As a result, the liquid becomes supersaturated with Si before nucleation. With increasing supersaturation, the nucleation barrier decreases, until solid Si finally nucleates and quickly captured most of the excess Si in the liquid in a rapid growth spurt (*10*). Subsequently, growth continues more slowly, at a rate determined by the steady external Si supply from the disilane vapor.

We explain this behavior with a simple kinetic model, in which the AuSi droplet and the growing solid Si nucleus are each assumed to maintain a constant shape. The rate of Si addition to the droplet is proportional to PA, where A is the exposed surface area of the droplet and P is the nominal disilane pressure (*19*). The droplets were treated as independent, consistent with annealing experiments that show that surface diffusion of Au and Si on the substrate is not appreciable over the time of the experiment (*20*). Nucleation occurs at a time t_n when the composition is c_n ($>c_0$). Once the solid nucleates, it grows rapidly, and we assumed that by the time it is large enough to be visible, the Gibbs-Thomson effect of interfacial curvature can be neglected. This means that the nucleus captures Si from the liquid at a rate proportional to $c - c_0$ per unit area.

From these assumptions, we derived (*17*) the following equation for the evolution of the linear dimension r of the Si particle with time, valid when r is small as compared with R:

$$\frac{dr}{dt} = k_{LS}\left[\alpha(c_n - c_0) + k_{VL}\frac{P}{R}(t - t_n) - \left(\frac{r}{R}\right)^3\right] \quad (1)$$

with initial condition $r = 0$ at $t = t_n$. R is the linear dimension of the AuSi droplet at the time of nucleation. The first term, $c_n - c_0$ in Eq. 1, reflects the initial growth rate at t_n. The second and third terms (P/R and r^3/R^3) represent the effect of c increasing because of Si addition from the vapor and decreasing because of Si capture by the nucleus. The three parameters controlling growth in Eq. 1 are the geometry-weighted supersaturation $\alpha(c_n - c_0)$ and the vapor-liquid and liquid-solid rate constants k_{VL} and k_{LS}, respectively (which also include geometric factors); details are given in (*17*). The geometric factors cannot be determined directly because we only have images of the droplets in projection.

Although the assumptions are highly idealized, we found that Eq. 1 gives an excellent description of the data, as illustrated in Fig. 2. We measured 33 nucleation events with droplet radii ranging from 6 to 24 nm, temperatures from 470° to 585°C, and pressures from 3.5×10^{-7} to 4.0×10^{-6} torr. The complete set of data, and fits to Eq. 1, are shown in fig. S1. It can be seen that Eq. 1 automatically captures and quantifies our qualitative observations regarding the role of system size and growth rate. It predicts that larger droplets give later nucleation with larger jumps. It also predicts that the crossover is sharper at lower pressure, which is confirmed by examination of the complete set of data and fitted curves. We initially fitted each curve independently and confirmed that the resulting values for k_{LS} and k_{VL} were consistent for all droplets at a given temperature T, as expected. The values for the geometry-weighted supersaturation, $\alpha(c_n - c_0)$, were, surprisingly, also the same. We therefore fitted the entire data set for each T with a single value of each parameter. Figure 3 shows the fitted values of k_{LS}, k_{VL}, and $\alpha(c_n - c_0)$.

The most dramatic aspect of the growth kinetics is the initial jump, which gives a direct visualization of the supersaturation as the nucleus captures the excess Si from the supersaturated liquid. Because the jump is quite sudden as compared with the incubation time and the subsequent slow growth, it is useful to consider Eq. 1 in the limit of large k_{LS}, giving

$$\frac{r^3}{R^3} \approx \alpha(c_n - c_0) + k_{VL}\frac{P}{R}(t - t_n) \quad (2)$$

In this limit, Si nucleates at t_n and "instantly" jumps to size $r = [\alpha(c_n - c_0)]^{1/3}R$. Subsequently,

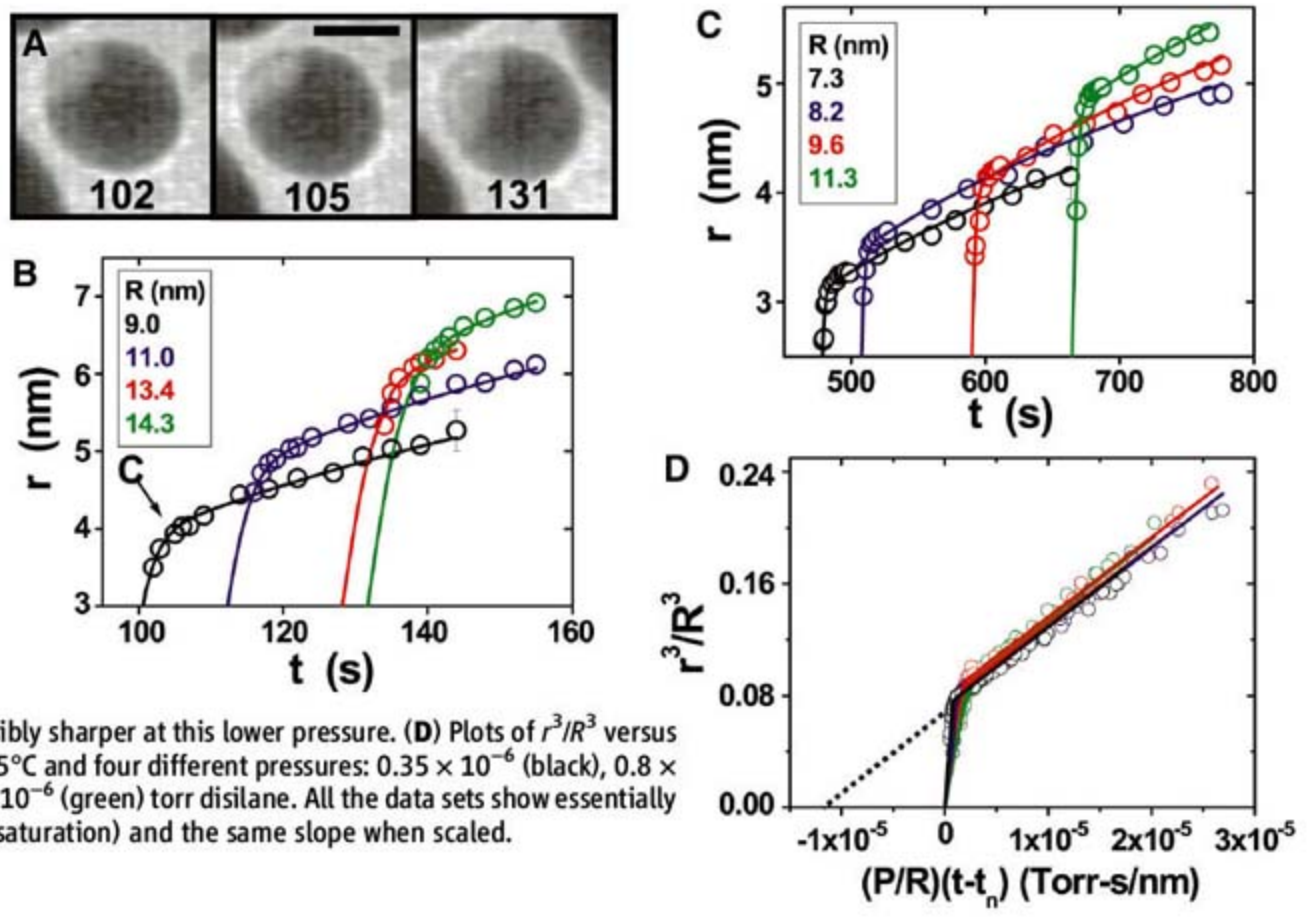

Fig. 2. (**A**) Images of a growing Si nucleus acquired at the times specified, recorded during deposition at 525°C and 4×10^{-6} torr. Scale bar, 10 nm. (**B**) Linear dimension r of several Si nuclei versus time t for droplets of different initial radius R (as indicated in the box) during the same growth experiment. Approximating the nucleus image by an ellipse, r is calculated as the geometric mean of the semi-major and semi-minor axes; that is, the radius of a circle with an equivalent area. The "C" marks the crossover point (see text) of the data set from the droplet shown in (A); the middle image was recorded at this time. Solid curves are fits using Eq. 1. The error bar indicates measurement errors of ~5%. (**C**) Plots and fits of r versus t at T = 525°C and $P = 8 \times 10^{-7}$ torr. In comparison with (B), the crossover is visibly sharper at this lower pressure. (**D**) Plots of r^3/R^3 versus $(P/R)(t - t_n)$ for all nuclei analyzed at 525°C and four different pressures: 0.35×10^{-6} (black), 0.8×10^{-6} (blue), 1.5×10^{-6} (red), and 4.0×10^{-6} (green) torr disilane. All the data sets show essentially the same jump (that is, the same supersaturation) and the same slope when scaled.